Long Term Membrane Potential (V_{mem}) Modulation and Cellular Senescence

A thesis submitted by

Bryan Young Jun Choi

In partial fulfillment of the requirements for the degree of

Master of Science

in

Biomedical Engineering

Tufts University

February 2015

Academic Adviser: Professor David L. Kaplan
Department committee member: Professor Qiaobing Xu
Cross department committee member: Professor Hyun Min Yi

Abstract

Endogenous bioelectrical signaling is a powerful system that controls various cell functions such as regeneration, proliferation and differentiation. This project specifically aimed to study the connection between modulation of membrane voltage and cell senescence. Human Mesenchymal Stem Cells of different passage numbers grown in depolarized/hyperpolarized conditions were tested in parallel to ascertain differences in varying phenotypes. Cell senescence characteristics were quantified by cumulative population doubling, changes in growth rate, attrition of telomere length and accumulation of tumor suppressor proteins P53, P21 and P16, which are often used as measures for the quantification of senescence.

The P53 protein pathway plays a pivotal role in regulating cell growth and apoptosis and is widely considered one of the most powerful tumor suppressor genes. The p21 pathway is called a cyclin-dependent kinase inhibitor that controls progression at G1 and S phases of the cell cycle. The p21 protein is a known mediator of cell cycle checkpoint regulation and DNA damage response. The p16 retinoblastoma pathway works to inhibit cyclin-dependent kinases leading to G1 cell cycle arrest through the retinoblastoma (Rb) protein.

In addition, the premature aging disease Hutchinson-Gilford Progeria syndrome was used as a model to better understand the connection between membrane voltage characteristics and cellular senescence. Experiments were conducted to measure how the Progeria syndrome may alter normal biophysical activity.

This project aimed to show how modulation of senescence with bioelectric signaling in human tissue might enable us to direct cell growth towards therapeutic uses.

Acknowledgements

I would like to give my most sincere thanks to all my committee members. Thank you for allowing me this opportunity to conclude my research work. Professor David Kaplan, thank you for providing me the opportunity and support to pursue research within your labs and within the Biophysical control group, as well as providing guidance throughout the program. I've learned so many valuable skills under your guidance and will always be grateful. Professor Hyun Min Yi, thank you for your support through both my undergraduate and graduate career at Tufts. You provided much needed timely/kind words of wisdom that got me through my years at Tufts. Professor Qiaobing Xu, thank you for your kind support and generosity with your time and wisdom.

I would like to thank the various members of the Kaplan lab/BME department that helped me through this process. I would especially like to thank Sarah for teaching me almost everything I know how to do in lab, giving me helpful guidance and insights, and answering all my stupid questions.

I would also like to thank the members of the Biophysical control group who would always be receptive to stop and provide helpful guidance—in the offices, labs and in meetings. A big thanks you to the regulars of 285, who were always open to joke/talk and discuss science!

Table of Contents

List of Figures and Tables

Chapter 1

Introduction

1.1 Project objective and scope

The overall goal of this thesis was to determine whether biophysical signaling plays an instructive role in the progression of cellular senescence. Cell senescence plays a commanding role in cell longevity, and is an important field of study that needs to be further investigated. It plays a functional role in the body, and is a process highly interconnected to a great number of known extrinsic and intrinsic forces posed on the cell. This study aims to connect the forces of biophysical signaling, which is a known regulator of cell behavior and function, with the onset of cellular senescence. Specifically, this thesis work studied the progression of senescence in successive passages of mesenchymal stem cells cultured in membrane potential modulating media.

Additionally, the biophysical characteristics of Hutchinson-Gilford Progeria Syndrome, the pre-mature aging disease, were studied to shed light on its role in disease progression kinetics.

1.2 Hypothesis and Project Aims

It is hypothesized that the depolarization of mesenchymal stem cells will somehow preserve the non-senescent, 'stem'-like features of pre-senescent cells. Conversely, the hyperpolarized conditions of the cells will see an early cell-cycle arrest and acceleration of senescence expression.

The attributes of senescence will be qualitatively observed by discernible phenotypes and quantitatively measured by the attrition of telomere length, changes in telomerase activity, and the expected expression of senescence markers. The expression of proteins seen in senescence will be measured throughout different passage numbers and culture conditions. The changes in telomere length, the incorporation rate of Bromodeoxyuridine (BrdU) into replicating DNA, as well as the expression of proteins ß-galactosidase and commonly used senescence "markers" p16, p21, and p53, will be used to measure senescence.

The aim of this project is to characterize how changes in polarization affect the onset of senescence. There have been no previous attempts to measure how biophysical control affects senescence expression, and this thesis work aims to understand how changes in membrane potential affect human mesenchymal stem cell senescence.

A secondary aim is to understand the bioelectrical characteristics of Hutchinson-Gilford Progeria Syndrome (HGPS). It is hypothesized that the change in the nuclear lamina caused by the HGPS syndrome also causes a change in the bioelectrical conditions, as measured by cell staining using the

voltage sensitive dye Bis-(1,3-Dibutylbarbituric Acid) Trimethine Oxonol ($DiBAC_4$-3). As HGPS causes symptoms of pre-mature aging, it is hypothesized that the HGPS cells will exhibit different membrane potential characteristics from control cells.

1.3 - Background in Senescence, Importance of Study

Some of the earliest observations of senescence were made in the culture of cells derived from explanted human tissue. It was observed that cells do not grow indefinitely, but reach a point where they trigger either proliferative arrest or apoptotic cell death programs.

In 1961, Leonard Hayflick measured and quantified a cell's limited potential to replicate, and coined the now famous term the "Hayflick Limit." Hayflick observed that different cells have predetermined proliferative potentials, and can only extend mitosis for set numbers of cycles. Hayflick then postulated that: "The finite lifetime of diploid cell strains in vitro may be an expression of aging or senescence at a cellular level (Hayflick, 1964)." The term cellular senescence referred here is defined as a cell's characteristic of long-term loss of proliferative potential, but with preserved metabolic function and activity. It should be noted that cellular senescence is distinct from quiescence, which is a reversible, and metabolically inactive state. Cell senescence may be divided into two categories: replicative and premature senescence. The latter involves the onset of senescence due to an external stress, such as oncogene-induced stress, or DNA damage caused by metabolic

stress or hypoxia (Kuilman, 2010). This type of senescence may be stopped to resume normal cellular proliferation once the stress inducing elements are removed. The former, which will be the topic of research in this thesis, is considered a part of the natural aging process to limit replication and the lifespan of a cell.

Though discovered by Hayflick and Moorhead in 1961, cellular senescence is still not a very well understood field of study, where relatively little is known about its molecular basis. This is partly due to the fact that cellular senescence is an incredibly heterogeneous and interconnected process, where many different elements are involved to create a highly evolved balance in machinery. The study of long-term change in membrane potential and the expression of senescence will help understand how biophysical control may be used to control the expression and onset of senescence.

1.3.0.1 Observable Morphological Changes of Senescence

Clear morphological changes are seen with the onset of senescence. The senescence response changes slightly depending on the type of senescence trigger, but generally become large, flat, and sometimes multinucleated. The large and flat phenotype is seen in most cells undergoing stress induced and DNA damage induced senescence (Chen et al., 2001). These changes can clearly be observed cross passage through phase contrast imaging.

Figure 0: *Changes in cellular morphology of human mesenchymal stem cells (hMSC) in early (A) and senescent (B) passages. With long term culture, hMSCs acquire a large and flat morphology as shown in figure B (Wagner, 2010).*

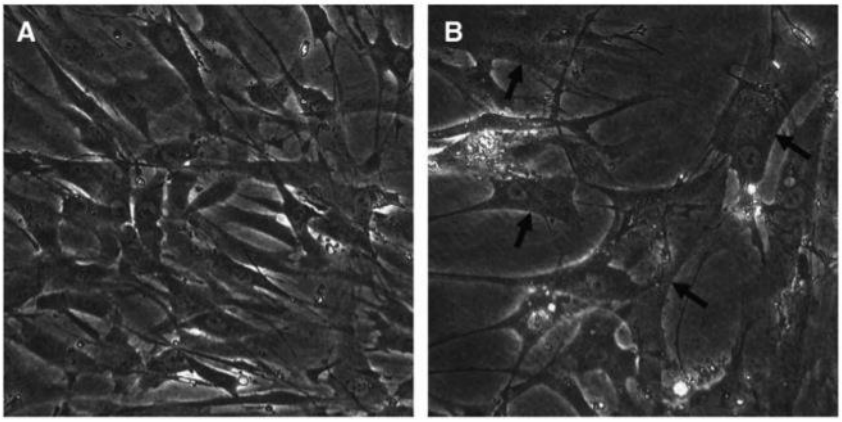

1.3.0 - Genomic Instability at the Root of Senescence

At the root of senescence is genomic instability caused by accumulation of genetic damage throughout an organism's life. Genetic integrity is constantly challenged by exogenous factors of biological, chemical, or physical nature and also factors intrinsic to the cell such as reactive oxygen species, spontaneous hydrolysis, and faulty DNA replication. The damages resulting from these factors cause changes in telomere length, telomerase activity, DNA point mutations, translocations, and general gene disruptions (Lord and Ashworth, 2012).

To compensate and counteract these activities and damages on nuclear DNA, the cell has an intricate system of DNA repair. This system involves both the control of telomere length, and the signal amplification

pathway cascade calling the DNA-damage response, which is activated upon detection of a discontinuation of a DNA double helix.

1.3.1 - DNA-Damage Response (DDR)

A discontinuation of a DNA strand instantly prompts a reaction by the cell called the DNA-damage response (DDR) to provide two clear functions: one, it prevents the duplication of a cell to prevent the passage of compromised genetic material into a daughter cell; and two, it prompts a swift response by the cell to coordinate repair DNA damage and preserve genomic integrity. These efforts are maintained in the cell cycle checkpoints, and once the DNA damage detected is repaired the cell resumes normal growth. If however, the DNA integrity cannot be recuperated, the cell responds by either inducing apoptotic death to remove the cell from the population altogether, or inducing cellular senescence, a response largely driven by the DNA-damage response (Fagagna, 2003).

Once a dsDNA break occurs, specialized complexes induces the employment of two large protein kinases ataxia-telangiestasia mutated (ATM), and ataxia telangiectasia and Rad3-related (ATR), at the site of DNA damage. With the introduction of these two protein kinases, a phosphorylation of the histone H2AX occurs to create γ-H2AX, a variant of the histone H2A with a C-terminal extension that allows it to employ non-homologous end joining to repair DNA. The protein γ-H2AX also then induces

a positive feedback loop to recruit greater numbers of ATM complexes, thereby increasing γ-H2AX concentrations in the chromatin (Fagagna, 2008).

The localized ATM activation induces the expression of γ-H2AX beyond just the damage site. When the minimum ATM threshold is passed, CHK2, a checkpoint kinase is activated, which is able to pass freely through the nuclear space to induce DDR signaling and expression of γ-H2AX all throughout the cell nucleus. The γ-H2AX is spread hundreds of kilbases away from the site of DNA damage to act as a ‘‘velcro’’ that attracts DDR-related molecules to produce cytologically detectable nuclei foci (Downey, 2006). These nuclei foci are thought to concentrate incidences of favorable protein-protein interactions and maximize the capabilities of DNA replication enzymes through optimal use of nuclear space.

Once a DNA lesion is repaired, the DDR foci are disassembled. However, if the DNA damage is substantial and harder to repair, the foci will stimulate even greater DDR signaling, thereby increasing the size of the foci and spread of γ-H2AX. This growth and spread of the DDR foci is an important aspect of senescence, as they take a large role in cell cycle checkpoint enforcement. Recent research studies showed that even in the absence of DNA damage, induced DDR pathways were adequate to induce cell cycle arrest (Sterigiou, 2004), to prove the DDR pathway plays a causative role in senescence.

Eventually, the DDR signaling pathway induces cell cycle arrest through expression of the tumor repressing protein p53, or inactivation of

the cell-division cycle 25 (CDC25) phosphatases. The cell cycle arrest via p53 expression leads to the creation of cyclin-dependent kinase inhibitor, p21, which produces a stable cell-cycle arrest. Conversely, the CDC2 inactivation is rapid in producing cell-cycle arrest, as these molecules are essential for cell division. CDC2 inactivation occurs more readily in onocogene related stress and DNA damage during the spindle assembly checkpoint (Bayart, 2004). Therefore, it is not as readily seen in normal senescence pathways.

With the development in the understanding of dsDNA breakage and the DDR response, γ-H2AX foci have been used in immunogenic assays to quantify DNA damage. In this thesis, the γ-H2AX protein was one of the different antibodies used to make a quantitative assessment of senescence. Immunofluorescence protocols reveal distinct speckled nuclear foci that stain brightly and sensitively. One fact that should be noted, however, is that the presence of speckled γ-H2AX staining does not necessarily mean the presence of DNA damage, but that of DDR signaling response (Ramirez, 2001).

1.3.2 - Telomere Length Management/Integrity of Cell

A telomere is a special type of nucleoprotein complex made of 7-20 kilbase pairs of tandem TTAGGG sequence repeats. They are thought to be protective mechanisms of DNA degradation, and a "cap" to the end of human chromosomes. Despite being composed of linear sequences of DNA ends, a telomere's double strand breakage does not activate the same response as

that of a DNA's double strand breakage. This may be due to a number of reasons—one of which being the unique structure of the telomere chromatin, and the other being the telomere associated DDR inhibition. Shelterin protein complexes, which are individually called telomeric repeat-binding factor 2 (TRF2) and protection of telomeres 1/2 (POT1/POT2), bind to double stranded telomeres and single stranded telomeres and prevent the activities of ATM and ATR, respectively (Lange, 2005). The TRF2 protein has the ability to remodel the end of telomeric DNA structure to create a higher-order t-loop formation to prevent distortions or untwisting of the DNA double helix. These shelterin proteins cap the telomeres to prevent the start of the DDR. Experiments conducted in the absence of these proteins showed that exposed telomeric sequences trigger DDR responses akin to that of a regular DNA breakage, and showed how shelterins provide a crucial protection function (Denchi, 2007).

It is well documented now that telomere shortening occurs with every cell division due to the ‘‘End Replication Problem.’’ This happens in every chromosome replication because the DNA replication process cannot be extended to the end of the strand, leaving a single-stranded overhang. A crucial component of DNA replication, Okazaki fragments, need RNA primers to attach ahead during DNA replication but due to the lack of space at the end of strand DNA replication becomes truncated. Through the iteration of this process, the telomeres slowly erode and shorten.

When the telomere length reaches a threshold length, the DDR is able to manifest even in telomeres. Senescence-related DNA damage foci (SDF) appear in the presence of shortened telomeric DNA to show ‘‘less than 20 but more than one’’ SDFs (Fagagna, 2008). To induce senescence, just one sufficiently short telomere is thought to have the ability to lead to the activation of ATM or ATR and checkpoint kinase inactivation. The specific length of the telomere tandem repeats is however, unclear.

1.3.3 - Telomerase Activity Between Cell

Although the telomere rate of attrition is nearly constant in cell division, the overall decrease of telomere length is different between cell types. Depending on the type of cell, there are varying activities of telomerase reverse transcriptase (TERT), which regulates the de novo synthesis of telomeric repeats to maintain telomere length. The presence and absence of telomerase has been found to tightly correlate to cell proliferative capacity. Inhibition of telomerase activity in immortal cancer cell lines lead to prematurely induced senescence, while conversely, the expression of it allowed extension of somatic cell lifespan (Kong, 2011).

The amalgamation of telomere length attrition and the TERT activities act as a molecular clock for different cells. Therefore, the elucidation of telomere length and telomerase activity throughout cell culture age is an important factor to consider for quantification of cell senescence. The change in the length of telomeres and activity of telomerase may indirectly shed light

on the onset of senescence in different culture conditions. Given the importance of these two factors in the expression of DDR and senescence, it was important to measure these factors. The telomere length and telomerase activity was measured through the different successive passages and culture conditions to ascertain how biophysical control, directly or indirectly affected these factors.

1.3.4.0 - Senescence and Cancer

Studies from the last two decades show that cellular senescence acts as an intrinsic failsafe mechanism of the body against cancer formation. For example, acute stress signals imposed by the inactivity tumor suppressor genes such as p53 and P16/RB, or the over activity of oncogenes have been observed to trigger the onset of senescence.

Initially, senescence was thought to be just an artifact of cell culture due to the difficulty of observation *in vivo,* but the detection of senescence expression in pre-malignant cancer lesions disproved this notion. *In vivo* systems of mouse and human research subjects showed that patients expressing incidents of cellular senescence and ‘‘hallmarks of senescence’’ in premalignant lesions had reduced malignant tumor growth (Dankort D, 2007). Conversely, cancer cells are typically devoid of typical senescence expression.

The undesirable phenotype response of senescence could be described as ‘‘antagonistically pleiotropic’’, as it promotes cell population

survival by promoting the cessation of cancer developments all the while limiting cell population lifespan and accumulating dysfunctional non-dividing, senescent cells (Campisi, 2005). Fundamentally, cell aging may be seen as a counterbalancing force that attempts to return to homeostasis from the cellular damage caused.

1.3.4.1 - Tumor Suppressors and Connection to Senescence

The tetrameric transcription factor and tumor repressor protein p53 regulates cell survival by controlling the cell cycle, DNA repair, apoptosis and the responses to cellular stress such as DNA damage, hypoxia, viral infection, and oncogene activation (Rufini, 2013). The transcription factor p53 is considered one of the most powerful tumor suppressor genes, and is often called the "guardian of the genome" for its role in inducing apoptosis and stopping cell proliferation of compromised cells (senescence).

Overexpression of the p53 pathway in mice caused accelerated aging, related ailments of age and greatly reduced lifespan. Therefore, the expression of p53 is considered one of the most crucial pathways in cellular senescence activation and an important protein to measure.

Under regular non-senescent conditions, the p53 expression remains low and undetectable due to its molecular instability. E3 ubiquitin-protein ligases such as MDM2, MDM4, COP1, and ARF-BP1 acts as a negative regulator of p53 by targeting it for proteasome mediated degradation. The introduction of stress disrupts the interaction between p53 and E3 protein

and stops the negative feedback inhibition of p53. Oncogenic stress activates p14ARF (product of CDKN2A locus) that covalently binds to p53, thereby preserving the molecule from degradation (Toledo, 2007).

Owing to its powerful ability to suppress oncogenic activity, the p53 is a common target for cancer therapies. In fifty percent of human cancers, p53 expression is suppressed or mutated, and many modern therapies involve the reactivation of p53 is cancer cells to stimulate p53-mediated apoptosis.

A downstream target of p53 is p21, also known as a cyclin-dependent kinase inhibitor 1 (CDKN1A). It binds to cyclin-CDK2/CDK1/CDK4/CDK6 complexes to control progression at G1 and S phases of the cell cycle. It's a known mediator of cell cycle checkpoint regulation and the DNA damage response (DDR). It is possible to get p21 expression without p53 activation, and this expression may also prevent cell proliferation and may contribute to cellular differentiation (Phalke, 2012).

Both the p53 protein and its downstream product p21 were measured to quantify senescence. It was important to include the p21 protein measurement in addition to that of p53, due to p53's molecular instability. Since p21 is not as dependent on proteasome-mediated degradation, it may prove to be a better target for measurement.

Figure 1: *This figure displays how the different endogenous and exogenous factors function to activate p53, and consequently p21. The image shows senescence/aging as a balancing power against the incidences of mutations, genomic damage, and consequently cancer (Vijg, 2009).*

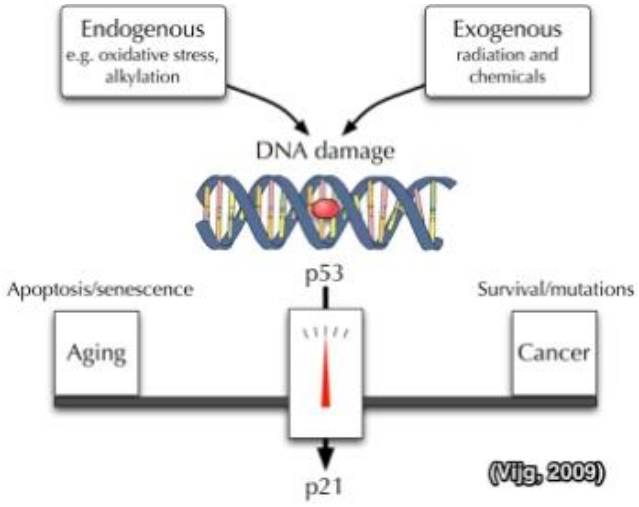

1.3.5.0 - Senescence Associated Heterochromatic Foci (SAHF)

Changes in nuclear heterochromatin in senescence are called senescence associated heterochromatin foci (SAHF). These foci can be observed through typical DNA staining methods such as DAPI staining and are distinct from the staining patterns of regular and quiescent human cells. The DAPI stained nuclei of senescent cells contain 30-50 brightly stained spots to distinguish itself from normal chromatin in cells (Narita et al., 2005). Additionally, since SAHF staining is distinct and is not associated with quiescent cells, the SAHF measurement may be associated solely with cellular senescence. The SAHF produced, which range from 0.6 to 1.6 μm or larger, are used to detect distinct changes in heterochromatin associated with senescence associated cell cycle exit.

The SAHF in senescence are formed from the compaction of chromatins in the chromosome and has a protective effect on the chromatin

to grant it nuclease resistance. These compactions target specific heterochromatin that contain proliferation-associated genes, such as E2F target genes, which are heavily involved in cell cycle regulation and DNA synthesis (Adams P, 2008).

Protein modifications such as histone methylation, which are typically seen in transcriptional silencing, are widely seen in SAHF. Histone methyltrasferases methylate the histones H3K27 and H3K9, which normally contribute to transcriptional activation, to form H3K27Me3 and H3K9Me3 (lysine 9-trimethylated-histone H3). The methylation of these histones instigates chromosome condensation and SAHF formation.

Suppression of enzymes such as histone methyltransferase lead to cells lines that are able to partially slow senescence. DNA methylation patterns of senescent cells suggest that phenotypes of mammalian aging are highly correlated to formation of SAHF and decrease in heterochromatin.

It should be noted, however, that SAHF formation is not a universal feature of cellular senescence. Though SAHF formation is seen in diverse cell types, SAHF formation is cell-type restricted (Kosar, 2008)

1.3.5.1 - P16 – Retinoblastoma pathway inhibiting cyclin dependent kinases leading to G1 cell cycle arrest

The action of a p16-mediated senescence is distinct from that of the p53 and DDR pathways, and acts through the retinoblastoma (Rb) protein pathway. Compared to the senescence attributed to p53/p21 expression, the

p16-retinoblastoma senescence pathway is a more rapid form of senescence (Schopfer, 2006). The Rb protein inhibits the function of cyclin dependent kinases and consequently controls the G1 to S cell cycle progression to prevent excess cell growth (Rayess, 2012). Senescence occurs with the inactivation of suppressor elements and the consequent enhancement of p16 expression. P16 based senescence is related to chromatin reorganization and suppression of genes such as E2F, similar to SAHF development. However, though SAHF development and p16 expression often happen in parallel, they form irrespective of each other (Kosar, 2011).

Since the p16 gene plays an important role in the regulation of the cell cycle progression, it is often used as a marker of oncogene activation and senescence. As such, the protein was also measured to be a target measurement marker for senescence.

1.3.6 - Nuclear Lamins and Laminopathies and Senescence

Changes and damage to the nuclear lamina can also lead to genomic instabilities. Nuclear laminas are vital parts of the nucleus that participate in genome stability and maintenance by tethering protein complexes and chromatin in the lamina. They are structural components of the nucleus, similar to that of intermediate filaments, forming a network mesh in the inner surface of the nuclear envelope. (Worman, 2010) Research interest in this field grew after researchers discovered that the basis of the Hutchinson-

Gilford Progeria Disease (HGPS) was an aberrant LMNA gene, which encode nuclear lamina proteins.

1.3.7 - Hutchinson-Gilford Progeria Syndrome

Hutchinson-Gilford Progeria Syndrome (HGPS) is a rare, genetic disease characterized by premature aging. The expression of Progeria is first characterized by failure to thrive, limited growth, full-body alopecia, and later expresses other age-related symptoms such as wrinkles, scleroderma, kidney failure, eyesight loss, atherosclerosis, and deterioration cardiovascular health. Patients with Progeria have small weak bodies, with characteristic loss of skeletal muscle and body, stiff joints, and other symptoms typically only attributed to the elderly. Patients of HGPS typically live only to their mid teens and early twenties, and at least 90% of patients die of complications associated to atherosclosis, such as strokes or heart attacks. Not surprisingly, arterial smooth muscle cells *mesenchymal stem cells*, and fibroblasts, in that order, express the phenotype of Progeria most dramatically (Danquah, 2013).

The cause of Progeria was found to be genetic mutation in the LMNA gene that produces four protein products—lamin A, lamin C, lamin AΔ10 and lamin C2. Typically, the lamin A molecule is first synthesized as a precursor molecule called pre-lamin A with a CAAX-box protein motifs (C – Cysteine, A – aliphatic amino acid, X – M/S/Q/A/C amino acids) at its carboxyl-terminus. A functional group called farnesyl then attaches to this CAAX-box motif to

guide it to the nuclear envelope. Once at the nuclear envelope, the farnesyl functional group detaches from the protein.

However, in patients with the Hutchinson-Gilford Progeria Disease, a *de novo* point mutation in the LMNA gene causes the LMNA gene to stop mRNA transcription early, resulting in an abnormally short protein variant of lamin A called progerin. This mutation of lamin A allows progerin to retain the CAAX-box motif but lack the proteolytic cleavage site for removal of farnesyl. Without the cleavage site, the farnesyl point group stays attached to the CAAX-box motif and accumulates along the nuclear envelope. The hydrophobic nature of farnesyl and incomplete connection between lamin A proteins induce the irregular bulging, of the nucleus. This mutation and blebbing of the lamin A leads to inadequate structural support and raises the potential for nuclear instabilities. These instabilities may be one of the factors leading to the premature aging phenotype of HGPS.

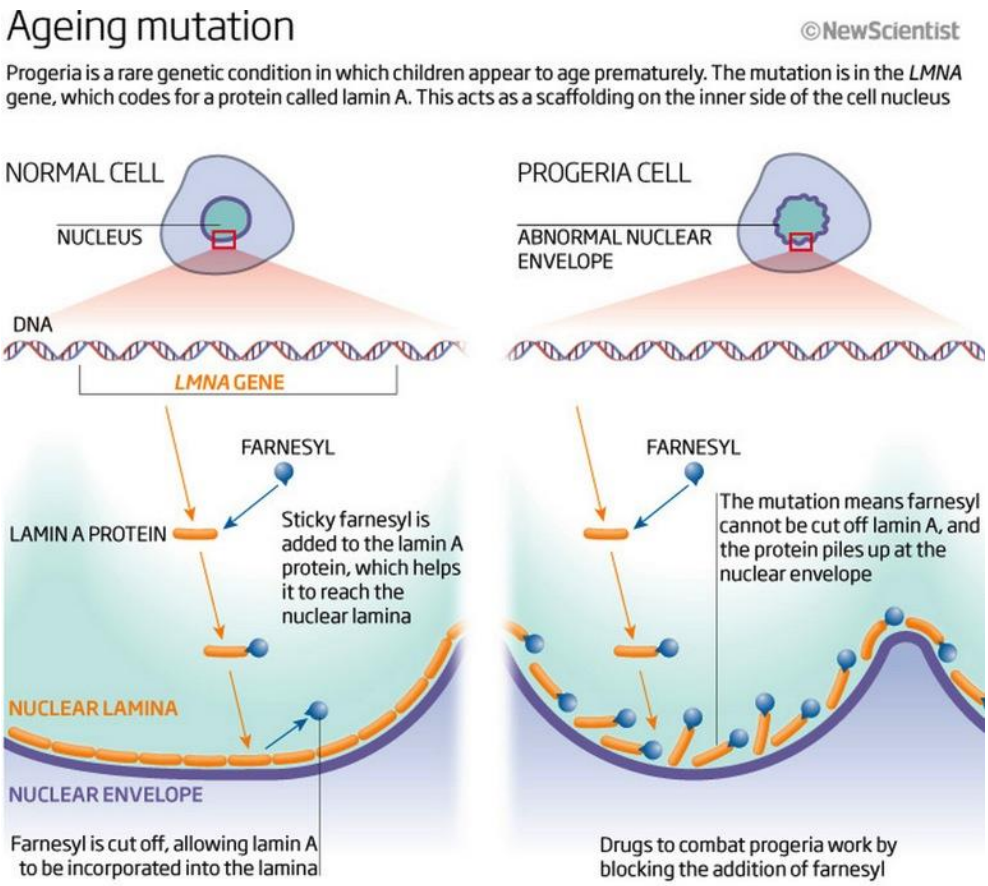

Figure 2: *The figure shows a representation of how a regular (left) LMNA, and irregular Progeria LMNA gene, create the nuclear lamina with functioning Lamin A and the mutated progerin protein (Miller, 2013).*

The mutations of nuclear lamina, and similar pathways that are expressed in Progeria have also been detected, albeit less dramatically, in the process of normal aging. The mutations of nuclear lamina have been seen to have a causal effect on p53 pathways, deregulation of the somatotrophic axis (major hormonal system regulating postnatal growth in mammals), and attrition of adult stem cells. This causal relationship was shown by the

decreased expression of prelamin A or progerin, and the resulting delay in "progeroid features" of HGPS mouse models (Prokocimer, 2013).

1.3.7.1 - Previous Progeria Experimentation and Senescence Expression

Using retroviral encoded (OCT4, SOX2, KLF4, c-MYC) HGPS fibroblasts cell lines, researchers were able to create HGPS-iPS cells that lacked progerin expression and recapitulated normal chromosomal integrity. Despite the clear and significant senescence phenotypes shown in HGPS somatic cells, HGPS-iPS cells were properly reprogrammed to effectively maintain pluripotency, and showed other "stem-like" characteristics similar to control iPSCs.

Unlike control iPSCs, however, once HGPS-iPS cells were differentiated to smooth muscle cells (SMC), the expression of progerin could be reactivated. These HGPS-iPSC derived SMCs were then serially passaged and tested for premature senescence phenotype. Serial passaging led to increased frequency of misshapen nuclei, loss of heterochromatin marker (H3K9me3), and showed at later passages (>passage 5) typical characteristics of premature senescence such as reduced telomere length, reduced # of Ki-67+ cells, and compromised cell proliferation.

It was then tested if progerin accumulation is the direct cause of "*accelerated*" cell senescence observed in HGPS-SMCs. Induced ectopic expression and accumulation of progerin in wild-type SMC showed compromised cell proliferation and nuclear defects as seen in HGPS-iPS

derived SMCs. Based off this, it shows that progerin played a large part in determining the phenotype of senescence in progeria cells. Study aims to understand how progerin plays a part in the expression of senescence.

A lentiviral vector with progerin-specific shRNA was then used to downregulate levels of mRNA, protein levels of progerin in HGPS-iPSCs then treated to differentiate into SMCs. This shRNA treatment showed marked improvement in proliferation capability as well as down-regulation of senescence related characteristics. Additionally, shRNA treatment of early passage HGPS-iPSC derived fibroblasts resulted in restoration of nuclear morphology and heterochromatin markers.

In addition to HGPS, a mutation in the LMNA gene causes a range of other diseases such as Mandibuoacral dysplasia, Dunnigan Type-Familial Partial Lipodystrophy, Emery-Dreifuss Muscular Dystrophy, and Cardiomyopathy. Characterizing Progeria in the context of biophysical control is important in understanding of the different diseases, and potentially finding new avenues to tackle the diseases.

1.3.8 - Biophysical Control Background

Biophysical signaling is a well-established regulator of cell behavior, cellular function, and plays a large instructive signaling role in cells. All cells, to varying degrees generate and receive bioelectrical signals as instructive cues for function. The different aspects of spatially distributed voltage gradients: Electric fields, ion flux, resting Voltage membrane potentials, are

more than a "housekeeping process" and carry instructive signals to moderate behavior at individual cell level and at tissue levels. In particular, trans-membrane voltage, which is the result of a combined effect of various ion channels and pumps under a concentration gradient and charge, has been shown to play an integral role in cell maintenance, mitotic activity, cell cycle progression, and differentiation (Levin, 2009).

The resting membrane potentials of cells have been seen to directly correlate with cell proliferative potentials, and cell "stem-ness". For example, cells with a higher degree of polarization (Hyperpolarized V_{mem}) tend to show more quiescent behavior and are less likely to undergo mitosis. Conversely, less polarized cells (Depolarized V_{mem}) tend to be cells that show more mitotically active behavior, such as various cancerous cells and precursor cell systems (Bingelli & Weinstein, 1986).

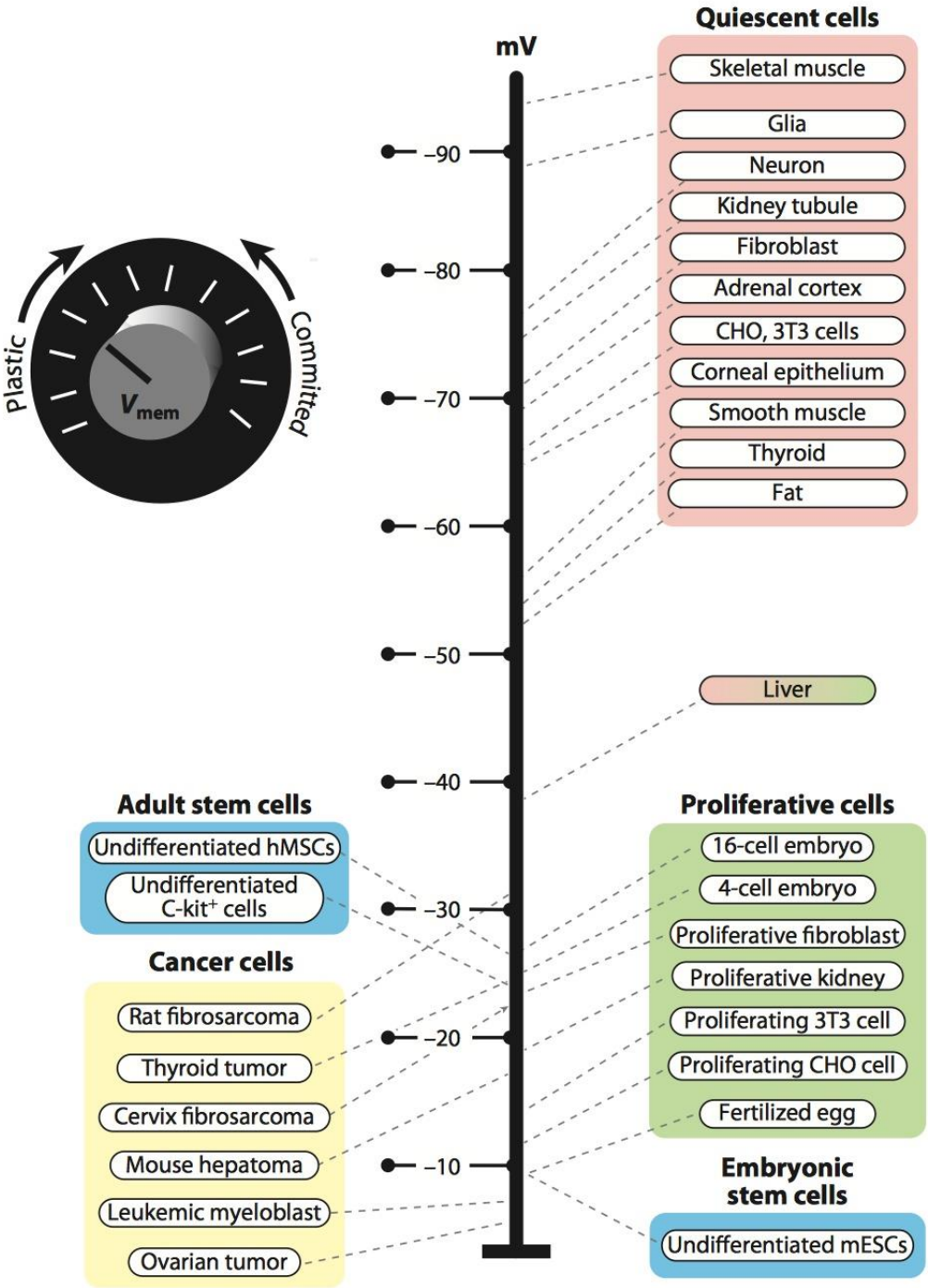

Figure 3 – *Shows how resting membrane voltage is a key parameter in cell behavior. Highly plastic cells tend to be depolarized; more mature terminally differentiated cells tend to be more hyperpolarized (Levin, 2012)*

Changes in voltage membrane potential have been related to changes in proliferation and differentiation in embryonic and stem cells. The K+ current channel is of particular interest in these systems, as it is required for DNA synthesis and regulation of proliferation. In mouse embryonic cells, for example, the blockage (hyperpolarization) of the delayed rectifier K+ currents (IK_{DR}) led to the inhibition of DNA synthesis and of proliferation (Wang et al., 2005). In Xenopus embryos, the depolarization induced by the disruption of an important K+ channel Kcnq1 (Kv7.1) activated neural crest regulator genes to cause a metastasis-like over-proliferation of melanocytes in the neural crest. Another study involving fully developed human epithelial monolayers showed that depolarization of cell membranes (via K+ channel inhibiting drug) was responsible for promoting proliferation and aided wound healing in the cell layer (Chifflet et al., 2005).

The results of these studies collectively show the importance of K+ channels in cell cycle regulation, and suggested strategies employing direct changes in membrane potential may reveal ways to coax cells back to expressing characteristics found in their developing and/or proliferative state.

1.3.8.1 - Biophysical Control and Therapeutic Roles?

In addition to altering cell quiescence, V_{mem} depolarization has been seen to be an instructive signal in controlling stem cell differentiation. *In vitro* cultures of hMSCs showed that the cells undergo hyperpolarization upon

osteogenic (-56 mV) and adipogenic (Vmem -74 mV) differentiation. And during this differentiation process, if the cells were forced to undergo depolarization, the osteogenic/adipgenic differentiation was downregulated. Conversely, if the cells procedure were hyperpolarized *during* differentiation, it up-regulated osteogenic differentiation (Sundelacruz, 2010). It was demonstrated that serial passages of hMSCs in culture led to decreased differentiation potential in osteogenic lineages and increased potential in adipogenic lineages. This was explained by the osteogenic lineages' greater sensitivity towards oxidative stress brought upon by cell aging than adipogenic lineages (Breudigam et al., 2010).

Furthermore, it was also observed how bioelectric cues could be used to override certain opposing biochemical signals. The depolarization of hMSCs allowed the cells to *disregard* the conflicting differentiation cues induced by insulin and dexamethasone, and maintain its pre-differentiated state. This points to the possibility that bioelectrical modulation could be used to ignore opposing chemical factors such as contact inhibition, and population pressures to maintain highly proliferative stem cell populations that promote therapeutic purposes such as wound healing and differentiation. Due to its ability to carry instructive signals and change cellular function, bioelectrical signaling has been looked upon as a promising avenue for therapeutics. Future works in this field will involve the use of pharmacological agents and genetic manipulation to engineer advantageous bioelectrical signals for tissue engineering.

The bioelectric environment governs the direction of stem cell fate, and has been shown to direct proliferation/'stem'-like behavior, differentiation, or generate cancer cell population. This introduction of the neoplastic phenotype was seen in the depolarization of human melanocyte cultures. This showed how bioelectrical signaling can "divert" the normal direction of growth to give rise to neoplasm. Then by extension, bioelectric modulation may be used as a tool *in vivo* to detect, prevent, or even control irregular cell cycles and tumorigenesis. In organisms such as planaria and salamanders, it has already been clearly observed that the bioelectricity underlying the regenerative capacity of these organisms could be manipulated to control regeneration. The more complete understanding of how bioelectricity controls cell systems could one day allow the use of bioelectricty as a platform for human tissue regeneration.

1.3.8.2 - Bioelectricty, Senescence, and Progerin

Progeria was an especially interesting model to study senescence and bioelectricity. Progeria cells *in vitro* express premature senescence and are implicated with the many characteristics of senescence such as genome instability, telomere attrition, and defective stem cell homeostasis (Burtner, 2010). To date, no investigations have been made in understanding the bioelectrical characteristics of Hutchinson-Gilford Progeria syndrome.

2.0 Rational Project Design – Methods of Measurement

As senescence expression is inherently a heterogeneous process in which multiple exogenous and intrinsic factors affect the outcome, it is naturally a difficult phenomenon to quantify. None of the biomarkers and assays used in quantification of senescence is sufficiently specific or unique as a 'marker' of senescence by itself. Furthermore, there is no standard biomarker used by researchers, since different cells express markers differently. There is unequivocal heterogeneity in the expression of senescence in long-term culture. Culture conditions such as contact inhibition and population density highly influence hMSC growth and affect the expression of senescence dramatically (Wagner, 2010).

In addition to providing highly standardized culture conditions to offset the obstacle of heterogeneous expression, multiple markers and assays were chosen in this thesis over multiple time points to best define and quantify the onset of senescence.

In addition, by defining senescence as a non-dividing, mitotically inactive state and using the two relationships as explained by Lawless et al. (2010) shown below, information could be extracted from cell counts to yield a growth curve that could estimate the proportion of proliferating cells and non-proliferating cells.

$$P \xrightarrow{r} 2P \qquad \text{Equation 1}$$

$$P \xrightarrow{A0\exp(kPD)} S \qquad \text{Equation 2}$$

Equation one represents the growth of proliferating cell giving rise to two progenitor cells. Equation two represents the change of a proliferating cell into a non-proliferating, senescent cell. The 'r' rate of proliferation of equation one is assumed to be constant number. The rate of senescence conversion of equation two was modeled as an exponential function dependent on the number of population doublings of the progenitor cells. The ordinary differential equations defining the dynamics explained above may be described as follows:

$$\frac{dP(t)}{dt} = rP(t) - A_0 \exp\big(kPD(t)\big) * P(t) \qquad \text{Equation 3}$$

$$\frac{dS(t)}{dt} = A_0 \exp\big(kPD(t)\big) * P(t) \qquad \text{Equation 4}$$

Then, with the known quantity:

LN(P) = rt; P = exp(rt)

$$PD(t) = \frac{\log\left(\frac{P(t)+S(t)}{P(0)+S(0)}\right)}{\log(2)} = \frac{\log(P(t)+S(t))}{\log(2)} \qquad \text{Equation 5}$$

With the algebraic equation and the differential equations derived, we are then able to derive the ratio of senescent cells versus proliferating cells.

Table 1 - Different Assays Used to Test Senescence Characteristics

Cell Line	Function	Type
hMSC	Cell Proliferation	BrdU antibody
	DDR	Gamma-H2AX antibody
	p21/p53	Cyclin-Dependent Kinase Inhibitor antibody
	SAHF	Compaction of chromatin
	ß-Gal Staining	Lysosomal ß-galactosidase staining
	Telomere Length	Flow Cytometry - PNA FISH/FITC

3.0 Materials and Methods

3.1 Materials

Abcam: p53 ms mAb (240); BrdU ms mAb (IIIb5); p21 ms mAb (wa-1); Ki67 rb pAb ab15580

Santa Cruz Biotechnology: p16 ms mAb (#B0912)

DAKO: Telomere PNA Kit/FITC, for Flow Cytometry (K5327)

Invitrogen: Pen-strep (#15240062), Alexa Fluor® 488 Goat Anti-Rabbit IgG (#A-11034), MEM Non-Essential Amino Acids 100X (#11140-050), DMEM GlutaMAX (#10566-016)

MatTEK: Glass Bottomed 24-well 13 mm (#P24-G-1.5-13-F), Glass Bottom 35 mm dish (#P35G-1.5-14-C)

Sigma Aldrich: $^{+}$Mg, $^{+}$Ca DPBS (#14040-133), Triton X- 100 (#T8787-50ML), Normal goat serum (#G9023-10ML), Bovine Serum Albumin (BSA, # A2058) World, 1301 Cell Line human (#01051619)

Corning Life Sciences: Cell Culture Plates 240well (#CLS3527)

Cell Signaling Technology: Senescence ß-Galactosidase Staining Kit #9860

3.2 Cell Culture

The hMSCs were isolated from bone marrow aspirate from a 25 year-old male donor and grown in successive passages in T-175 cm^2 in control growth media composed of: 500 mL – Dulbecco's Modified Eagle Medium (Invitrogen); 50 mL – Fetal Bovine Serum (Invitrogen); 5 mL - 100X

Concentrated Penicillin-Streptomycin (5,000 U/mL); 5 mL – 100X MEM Non-Essential Amino Acids.

For the high potassium (depolarized) cell condition, potassium gluconate was dissolved to 1 M and filtered to create a sterile solution. Approximately 1 mL was used per 25 mL of control medium to achieve a final potassium concentration of 40 mM.

For the pinacidil (hyperpolarized) cell condition, pinacidil monohydrate was dissolved in ethanol to create a 50 mM solution. Approximately 50 μL was used per 25 mL of control medium to achieve a final pinacidil concentration of 2 μM.

The cells were kept in a humidified 37 degree Celsius, 5% low-oxygen and 5% low-CO2 incubator. Fresh media was given every three days. The cells were passaged when they reached roughly 80% confluence to minimize effects of contact inhibition on senescence expression.

3.2.1 Cell Trypsinization, Spin-Down Procedures

The cells were trypinsized in 0.25% trypsin-EDTA with phenol red (Invitrogen). After approximately five minutes of incubation, the cells were detached and collected for pelleting procedures. If the cells were not completely detached after five minutes, the flasks were tapped to completely detach cells from the culture flasks. Small collections of the cell-media solution (~100 μL) were collected to count during the spin-down procedures.

The cell-media solutions were spun at 500 g and kept at 4 degrees Celsius. Once the cells were pelleted, the media was removed. The cells were then either re-plated to a new flask or saved and frozen in a FBS solution containing 8% dimethyl sulfoxide (DMSO).

3.2.2 Cell Counting/ Seeding/Freezing Procedures

The cells in the media were counted using a hemocytometer. Each trypsinized cell line was counted at a minimum of six times to ensure an accurate and reliable cell count.

Once the number of cells was determined, the cells were seeded at 5,000 cells/cm^2. For a T175 cm^2 flask, approximately 0.9 to 1.0 million cells were seeded to maintain constant cell density through different passages. In cell plating for analysis, approximately 5,000 cells/cm^2 were used and allowed to adhere completely for analysis. Due to the possibility of contact inhibition affecting cell growth, a near constant seeding density was necessary for this experiment.

Cells were frozen at approximately 1.0 x 10^6 /mL of FBS solution with 8% dimethyl sulfoxide (DMSO). The cells were frozen in -80 ^oC overnight in a cryobowl, and then transferred to a liquid nitrogen bath.

3.3 Viral Plasmid DNA

The viral plasmids were ordered from Addgene (pCDHblast MCSNard OST-LMNAd50 and pCDHblast MCSNard OST-LMNA**)**, and were specifically

ordered without GFP to allow for DiBAC4 staining. GFP and DiBAC4 share similar excitation/emission profiles, and therefore were not suitable for analysis.

3.3.1 Plasmid DNA Isolation

A single bacterial colony were streaked and isolated on LB agar plates (40 g/L) with ampicillin for bacterial selection. The single colonies were grown in a shaker flask with 50 milliliters of ampicillin-enriched media and allowed to grow (37ºC, 250 RPM) for approximately 6 hours. The grown bacteria was then pelleted by centrifugation and processed for DNA isolation via Qiagen Mini-Prep.

The pelleted bacterial cells were first suspended in an alkaline lysate buffer that contains NaOH/SDS alkaline solutions that solubilizes phospholipids and protein components of the cell membrane to induce cell lysis and release cell contents. Then, the lysate was neutralized and adjusted to high salt concentration that causes denatured cell debris, chromosomal DNA to precipitate, while allowing smaller plasmids to renature and stay in solution (“QIAGEN Miniprep,” 2006). This solution was then re-pelleted to separate the plasmid DNA containing supernatant from the unwanted precipitant pellet.

The supernatant was then loaded onto a silicon adsorption column and treated with a series of different wash chemicals to remove non-DNA contaminants. The MINI-prep protocol effectively separates the

chromosomal DNA and proteins from plasmid DNA. In the end, a concentrated solution of DNA in elution buffer remains.

3.3.2 DNA Sequencing

To ensure that the proper DNA was isolated for lentivirus production, the DNA was sequenced. The sequencing was processed through an external company called GENEWIZ. The sequence yielded was analyzed using the Basic Local Alignment Search Tool (BLAST) provided and cross-referenced to the NIH database. For the Progerin and Lamin A expressing DNA, 99% identification to the source plasmid was observed.

Table 2 – Sequencing Results

Plasmid	Max Score	Total Score	Query Coverage	Identification
LMNAd50 (Progerin)	1698	1698	87%	99%
LMNA (Lamin A)	1618	1618	86%	99%

3.3.3 Lentivirus Creation

Lentiviruses for Progerin and Lamin A transduction was outsourced to the Viral Vector Core of the Main Medical Center Research Institute. Approximately 50 micrograms of each DNA samples were sent to create the lentiviruses. Five hundred microliters of 100x concentrated viruses were received.

3.3.4 Transduction Procedures

Approximately 3 μL per cm^2 were observed to create good transduction efficiencies. The concentrated virus solution was delivered via DMEM media, and allowed to transduce for 48 hours for optimal transduction. Following transduction, the cells were washed in PBS two times, and then media containing was changed every 24 hours for 1 week.

3.3.5 Puromycin Selection, Kill Curve

The lentiviruses were designed so that they were sensitive to puromycin, the aminonucleside antibiotic. A kill curve selection process was used to determine the minimum puromycin concentration to select properly transduced cells. The cells were seeded at roughly 25% confluence, and tested with working concentrations ranging from 0.25 to 10 μg/mL. The cells are kept in different working concentrations of the antibiotic and observed until they died and detached. The optimal, minimum dosage for selection concentration was determined to be roughly 2 μg/mL. This concentration was used for the cell culture medium going forward.

3.3.6 Horizontal Transfer

To ensure that the cells were not producing viruses, horizontal transfer procedures were conducted alongside regular transduction. Following the second wash, the media in the transduced culture was collected and placed in a fresh plate of cells. From here on, cell culture

procedures follow normal transduction procedures. It was observed over 10 days if the cells remain alive or die due to the lack of puromycin resistance. If the results of these tests were negative and the cells with the transferred medium die, it was determined to be safe to culture the cells in non-viral approved conditions.

3.4 Imaging

3.4.1 Brightfield Imaging

An inverted Leica fluorescence microscope was used to obtain phase contrast images. Phase contrast images were used to make qualitative observations of different cell lines, and conduct quantitative analyses for assays such as the X-Gal ß-galactosidase assay.

3.4.2 Fluorescent Imaging

A 490-505 nm, 500-550 nm, and 450 nm filters were used to view the Goat anti-mouse TxRed secondary antibody, the Goat anti-rabbit FITC secondary antibody, and the DAPI DNA staining, respectively. A black and white camera was used due to its greater sensitivity, and color was added in image processing (TxRed – Red, FITC – Green, DAPI – Blue).

3.4.3 Confocal Imaging

In addition to bright field and fluorescent imaging, fluorescence confocal microscopy was used to yield more detailed images. This was important especially for the Progeria cells, as it was important to observe

clear differences in nuclear lamina shape and cell membrane outlines for $DiBAC_4$ dye staining.

3.5 Immunohistochemistry (IHC)

To evaluate different cell lines' protein expression, seeded cells were evaluated for antibody staining under fluorescence and confocal microscopy. The cells were first rinsed in DPBS and allowed to equilibrate for five minutes. Then, under a fume hood, the PBS solution was removed and the cells were fixed in 10% formalin for approximately 10 minutes. The formalin solution was removed and carefully disposed in the appropriate waste containers. The cells were then washed 3x for 5 minutes each in DPBS. The cells were then blocked and permeablized in a DPBS solution containing 5% goat serum, 0.3% Triton-X at room temperature for approximately one hour. The cells were then washed again 3x for 5 minutes each, then incubated with the primary antibody solution overnight in 4 degrees Celsius. The primary antibody solution consisted of 1% FBS, 0.3% Triton-X, and varying concentrations of primary antibodies, depending on its protein binding affinities (p16 – 1:100; p21 – 1:200; p53: 1:200; BrdU: 1:200). Once fully incubated, the cells were washed and incubated with the appropriate secondary antibodies for three hours at room temperature. The secondary antibody solution used a 1:1000 dilution of antibody to PBS. Following the secondary antibody staining, the cells were washed again. The cells were

DNA counterstained with a 300 nM DAPI solution in PBS for approximately 2 minutes, then rinsed for sample viewing.

3.5.1 BrdU Labeling/Fixation

The procedures for the BrdU staining were slightly different, as it first required BrdU incorporation and then specialized treatment to expose nuclear DNA. The BrdU was first incorporated over twelve hours in a 10μM working solution of media. After formalin fixation, a NaOH/Sodium tetraborate protocol was used. Then cells were washed (2x 5 minutes), and then treated with 0.01 N NaOH solutions for 10-15 seconds. Then, a 0.1 M sodium tetraborate solution was added for 5 minutes to neutralize the basic solution. The cells were then washed (1x).

3.5.2 Senescence associated heterochromatin foci (SAHF)

Senescence associated heterochromatin foci (SAHF) were calculated as DAPI integrated intensity gradient, as measured by a protocol explained by Passos et al. Using a ‘‘differentials’’ ImageJ plugin, the nuclear region of interest was observed as a measure of granularity. The filtration procedures showed the ‘‘granularity’’ characteristic of nuclear DNA and separates SAHF-positive cells from non-granular cells, yielding a percentage.

3.6 Functional Assays

3.6.1 Beta-Galactosidase Activity with Cell Senescence Progression

Probably the most reliable and widely used ‘‘marker’’ for senescence is the senescence-associated ß-galactosidase (SA-ß-gal) assay. It is a colorimetric assay that allows for detection of ß-galactosidase, an enzyme is detectable in cells undergoing induced or replicative senescence due to increased lysosomal ß-galactosidase content. ß-galactosidase catalyzes the hydrolysis of ß-galactosides to simple sugars at a pH of 6.0.

For this assay, an artificial ß-galactosidase substrate, which consists of a galactose molecule and an ‘X’ group dye, was added to be catalyzed by ß-galactosidase at a pH of 6.0. The enzyme cleaved the X-gal to yield galactose and an ‘X’ group dye that reacted with oxygen to precipitate into a blue dye. This process stains senescent cells the characteristic blue color to distinguish them from proliferating cells. Currently, the molecular basis behind why senescent cells more readily express ß-galactosidase activity is not known. However, the general phenomenon of increased lysosomal number and activity with aging and replicative senescence has been long established (Robbibs et al., 1970).

In addition to the event of staining (overall percentage), the degree of staining (stain area percentage) was also an important factor in measurement/quantification of senescence. At a certain point in culture, most, if not all cells may show the blue senescence staining. However, the degree of staining and the percentage of the cell the blue covers will vary.

Therefore, it was necessary to take note of the coverage of cell staining in addition to the numbers of cells stained.

3.6.1.1 Cell Seeding Density

Before proceeding with this assay, it was important to completely thaw all reagents. The X-gal solution used in this assay has a tendency to form aggregates and 'clumps' that interfere with the visualization of stained cells. Therefore, the solutions used were thawed for a minimum of 1 hour at 37 degree Celsius. Once the reagents were thawed, the staining mixture was first created: 1 mL staining solution, 125 µL Reagent B, 125 µL Reagent C, 0.25 mL X-gal solution, 8.5 mL ultrapure water. This solution was filtered using a 0.22 µm filter due to potential aggregates in solution.

The target cells were washed in PBS then, approximately 0.15 mL/cm2 of the given fixation buffer (20% formaldehyde, 2% glutaraldehyde, 70.4 mM Na2HPO4, 14.7 mM KH2PO4, 1.37 M NaCl, and 26.8 mM KCl) is added and allowed to fix for 6-7 minutes at room temperature. These cells were then washed three times in PBS, then 0.1 mL/cm2 staining mixture was added and incubated at 37 degree Celsius in an incubator WITHOUT CO2 for approximately six hours (optimized). This was important because ß-galactosidase is pH dependent, and therefore, the assay could not be incubated in a CO2 enriched atmosphere.

Following incubation, the cells could be observed and counted to calculate the percentage of senescent cells in culture. If aggregates appear, the cells were incubated at 37°C ~30 minutes to dissolve protein clumps.

3.6.2 Flow Cytometery based FISH FITC-PNA Relative Telomere Length Measurement

The telomere length was measured by a high throughput flow cytometery based method. The assay used fluorescence in situ hybridization (FISH) methods and used fluorescein (FITC)-conjugated peptide nucleic acid (PNA) to obtain the relative telomere length (RTL) as compared to a control cell line. The PNA used were analog to the TTAGG repeating sequences of telomeres, and binded accordingly. The control cell line used here was the 1301 cell line, a human T-cell leukemic cell known for its tetraploidy and long telomere length. For consistency, large numbers of the 1301 cells were first grown and frozen for use with this assay.

The assay used denaturation, hybridization, and DNA staining steps to obtain the RTL value. In two separate tubes (control, sample), an equal number of control and sample cells were first placed, and then washed. The cells were subjected to a high temperature (82°C) to denature DNA, and then allowed to hybridize (40°C) with PNA. To the one tube used as the ‘‘control,’’ PNA probes lacking FITC probes were added, then allowed to hybridize. In the other sample tube, a PNA probe with the FITC probes were added to show fluorescence amounts directly corresponding to the amount of

telomeres. Finally, a DNA staining solution containing propidium iodide was added to distinguish the tetraploid control cells from the diploid sample cells.

The samples were analyzed through a graph comparing FL1-H (FITC staining) vs. FL3-H (DNA ploidy). By considering the difference in FL1-H intensity between the control (w/o FITC-PNA) and the sample (w/ FITC-PNA) and using the following equation, the RTL was calculated.

$$\text{RTL} = \frac{(\text{mean FL1 sample cells with probe} - \text{mean FL1 sample cells without probe}) \times \text{DNA index of } \textbf{control} \text{ cells} \times 100}{(\text{mean FL1 control cells with probe} - \text{mean FL1 control cells without probe}) \times \text{DNA index of } \textbf{sample} \text{ cells}}$$

Equation 6

3.7 Measurement of Membrane Potential $DiBAC_4$ Dye

The membrane potential between two different lines of cells may be compared using $DiBAC_4$ dye staining. This anionic dye works by diffusing more readily into more depolarized (less negative) conditions, compared to hyperpolarized (more negative) conditions. The dye binds to the intracellular membrane and proteins to show fluorescence, directly correlating to polarization levels. Approximately 10 images were taken per 35 mm glass-bottomed MatTek well dishes. Background images were taken and subtracted from the original image to reduced background noise.

This dye could be used in both a high-throughput manner through flow cytometery and immunofluorescence-based imaging. The flow cytometer based method is useful to understand the overall cell population characteristic in a more highthroughput manner, showing how whole

populations exhibit overall values of membrane polarization. The immunofluorescence based image analysis is useful to determine the membrane polarization of single cells in culture.

The suspended cells and adherant cells were incubated in a working solution of 1.25 nM of $DiBAC_4$ for approximately 15 minutes, and then processed for analysis. DiBAC4 was a moderately temperature sensitive dye, therefore, time/temperature was standardized in these experiments and conducted at low sample numbers.

3.8 Image Analysis

Care was taken to minimize possible bias introduced in image analysis. To obtain accurate measurements and cell counts from image analysis, the images from the same staining were all subject to a threshold/filter level for all images, and not at a image by image basis. In addition, blackfield background images were subtracted from the image using ImageJ, taken in all control images.

For the analysis of $DiBAC_4$ staining cell borders (without the nuclei) were outlined with polygon selections to measure the average pixel intensity of staining. The pixel intensity readings were obtained on a well-to-well basis, and then averaged to obtain a cumulative value.

3.9 Statistical Analysis

3.9.1 Histological Analysis

Samples for all histological analyses were analyzed at a minimum of n=6 for different staining populations. A minimum of ten images of these replicates were collected and analyzed to show representative differences among varying treatment groups. Measures of staining intensity, cell size, area were calculated using ImageJ's toolbox. Statistical analyses were performed with Microsoft Excel, Matlab and FlowJo.

3.9.2 Graphical Presentation of Data

For purposes of accurate analysis and representation, the results of histological assay were presented in the form of two graphs—one in percentage stained vs. days, the other in percentage stained vs. cumulative population doubling. As explained earlier, since culture condition factors such as contact inhibition, population density and overall cell growth influence expression of senescence characteristics dramatically, it was important to normalize senescence marker expression to cumulative cell growth (population doubling) (Wagner, 2010). Moreover, this form of data representation is a standard form of data representation in studies of senescence and aging.

3.9.2.1 Limited Population Doubling Data Set

It should be noted that the population doubling analysis was only performed using one data set. Therefore, error analysis could not be performed. However, the general trend of growth collected from the partial data sets of pre-senescent cultures, mirrored the behavior of the observed data set shown above.

Furthermore, the smaller cell population data did not allow for a clear representation of the different cultures' respective cell growth rates. Therefore, a moving average calculation was used to remove irregularities and to better discern an underlying trend. The moving average was calculated using the Microsoft Excel data analysis toolbox and obtained from the following equation:

$$MA(t) = \frac{GR(t)+GR(t-1)+GR(t-2)}{3} \qquad \text{Equation 7}$$

As the above equation uses the average of two previous ($GR_{(t-1)}$ and $GR_{(t-2)}$) and current ($GR_{(t)}$) growth rate data point to obtain a moving average, the graph of the growth rate moving average starts at the third observed data point.

4.0 Results

4.1 Data Analysis

As discussed previously, hMSCs were grown in different media conditions until ~80% confluence, then frozen and/or passaged according to passage number. The cultures were never allowed to reach full confluence to minimize cell-cell contact inhibition and to allow for optimal growth of cells. The cells were frozen to minimize cross-passage variability upon thawing/seeding procedures and to provide similar culture conditions prior to testing. The cells were first thawed into T175 flasks, and then seeded onto 24-well plates (~5000 cells/cm^2) for testing. Below were the passage numbers chosen:

Table 3 – Culture Conditions and Time in Culture

Culture Conditions	Passage Number (Days in Culture)				
Control	1 (0)	5 (22)	10 (63)	15 (133)	-
High Potassium (Depolarized)	-	5 (22)	10 (58)	15 (103)	20 (187)
Pinacidil (Hyperpolarized)	-	5 (22)	10 (62)	12 (102)	-

The different cultures gradually acquired the characteristics of senescence, and then eventually entered replicative senescence at later passages. This transition into senescence could be visibly observed by the acquisition of the

characteristic enlarged and flattened cell morphology of senescence, as wells as a clear decrease in cell growth kinetics.

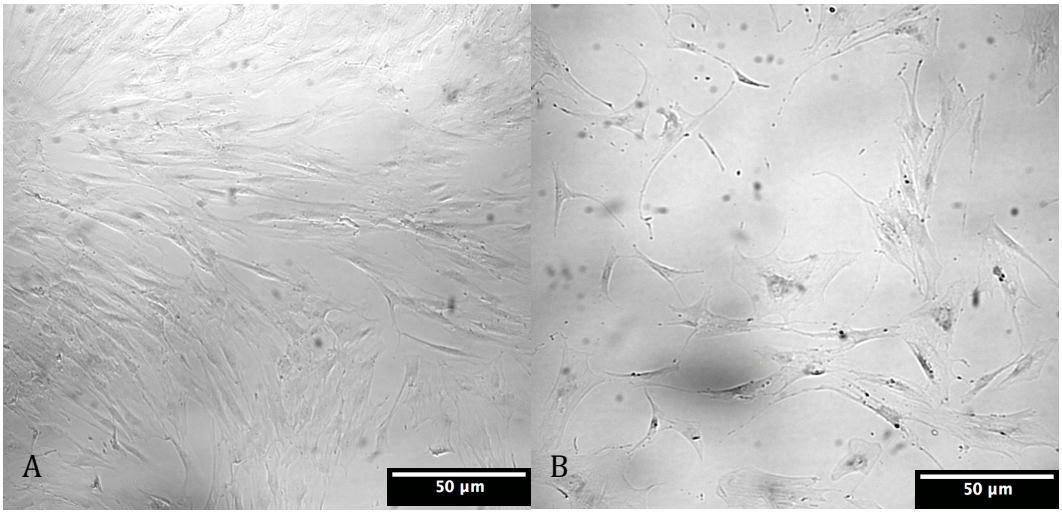

Figure 4A/B*: Bright field images comparing the different morphologies acquired with senescence. The left image shows passage 1 cells approximately 4 days in culture, and the right image shows cells cultured for 110 days, exhibiting the larger volume, flattened cell morphology.*

4.2 Population Doubling

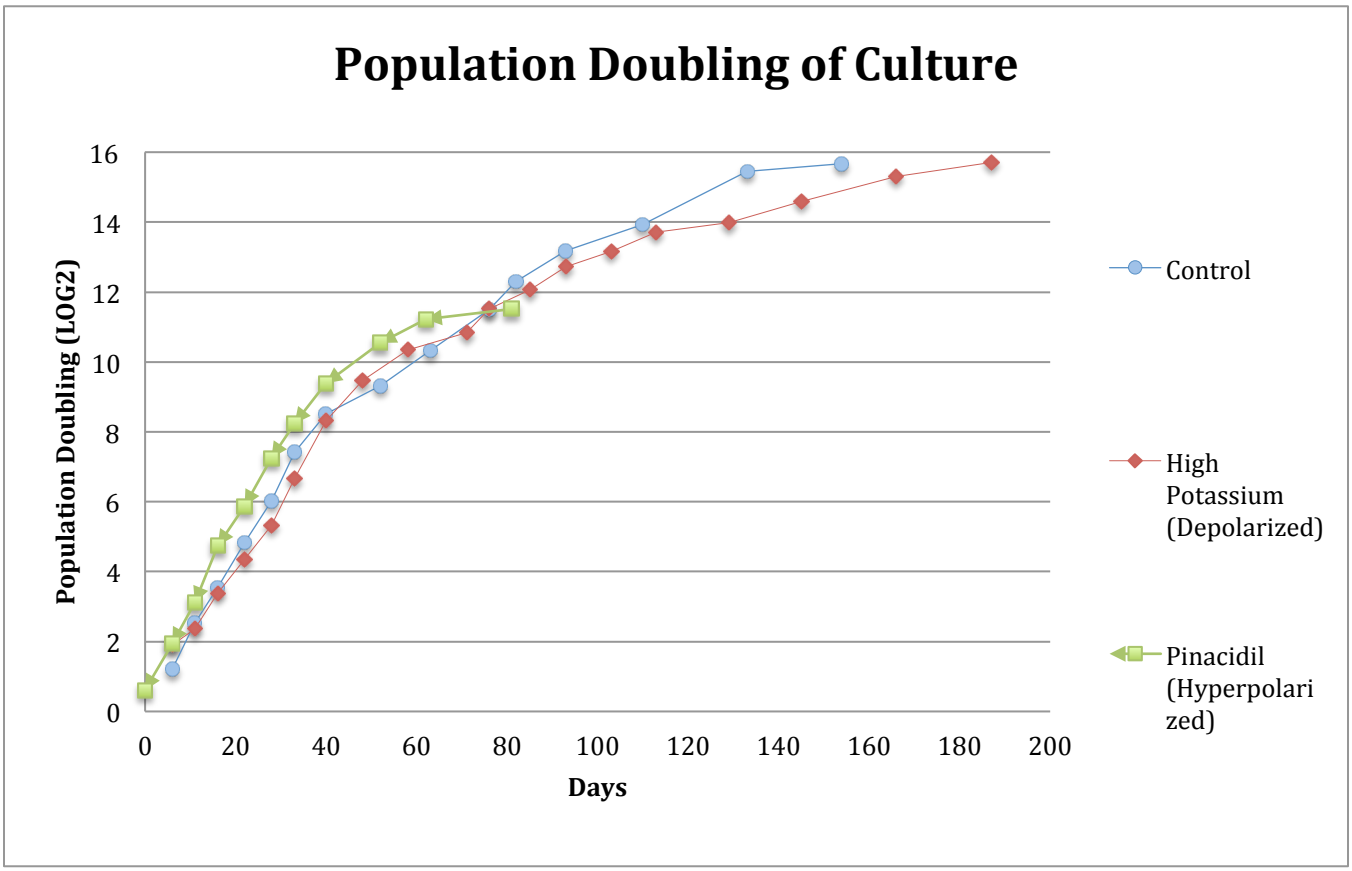

Figure 5: *The figure above shows the overall population doubling of cells in culture until complete replicative senescence. The final PD values for depolarizing high potassium medium, hyperpolarizing pinacidil medium, and control medium yielded population doublings of 15.7, 11.5, 16.3 and respectively.*

Population doubling data was obtained from the measurements of cell population number through different passages and time points, then calculated by the following equation:

$$PD(t) = PD(t-1) + \frac{\log\left(\frac{P(t)+S(t)}{P(t-1)+S(t-1)}\right)}{\log(2)} \qquad \textit{Equation 6}$$

Flasks were allowed to grow for a maximum of three weeks in culture, and if the culture did not grow to the desired confluence, the population was deemed non-proliferating and senescent.

Prior to the population doubling calculations, it appeared that the depolarization of mesenchymal stem cells prolonged cell division and preserved a more proliferative state. The depolarized cells grew for approximately 50 days longer than control cell conditions, and appeared to hold greater proliferative capacity towards later passage numbers. However, the normalization of growth to population doubling values showed that the control media conditions yielded a higher final PD value before growth arrest.

The final PD values for depolarizing high potassium medium, hyperpolarizing pinacidil medium, and control medium yielded population doublings of 15.7, 11.5, 16.3 and respectively.

The control conditions had a higher value of final population doublings than both the depolarized and hyperpolarized conditions. Though the difference in PD was not drastic between the depolarized and control cell lines, it was seen that the population growth was slowed by long term culture of cells in membrane depolarizing media. In addition, hMSCs cultured in

hyperpolarizing pinacidil medium showed significantly earlier cell cycle arrest and overall decrease in cumulative PD.

4.3 Calculated Growth Rate vs. Days in Culture

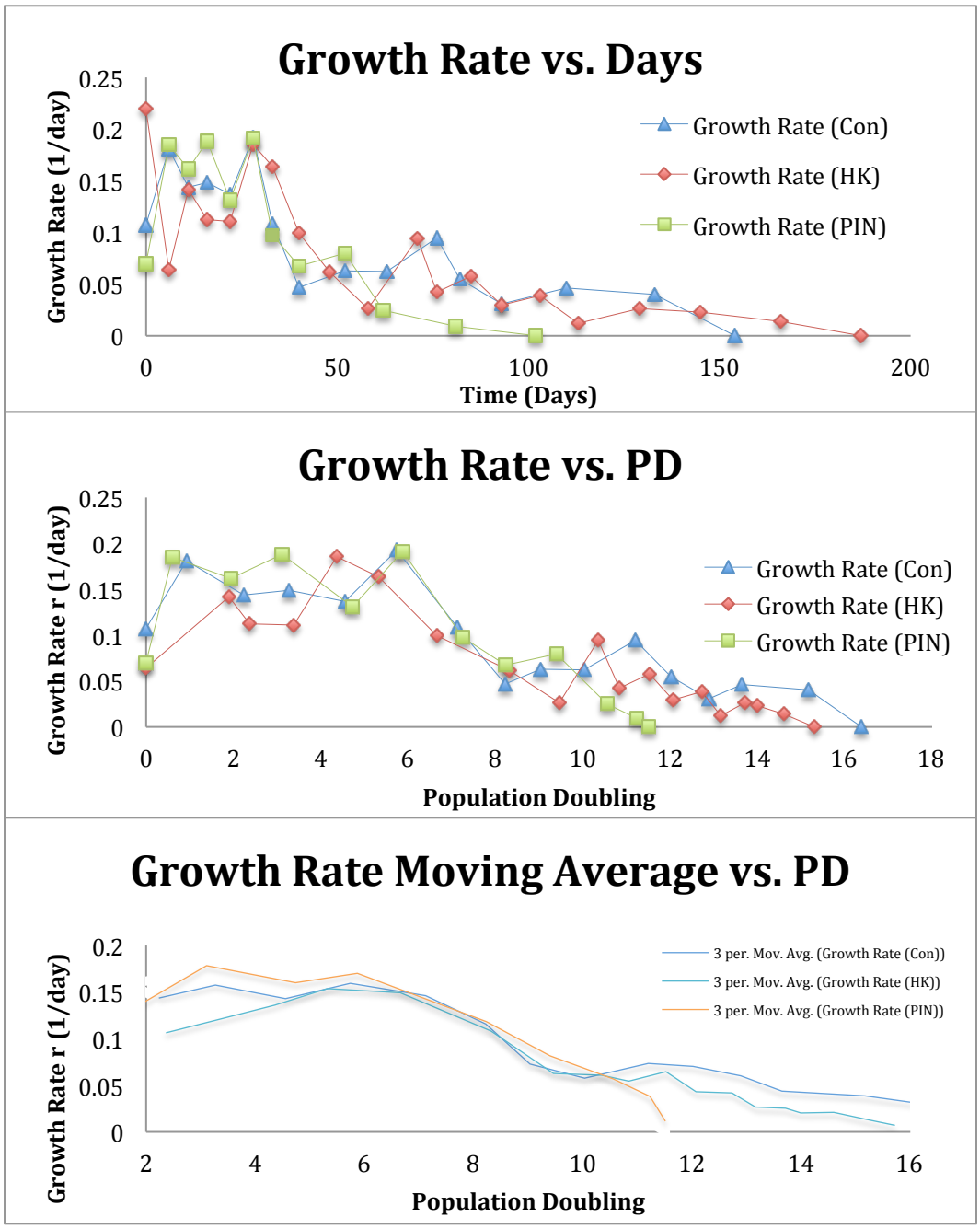

Figure 6 (top) 7A/B (bottom): *The growth rate of control (CON), depolarized (HK), and hyperpolarized (PIN) conditions were first compared to days in*

culture in figure 6, then normalized to population doubling values in figure 7A. Figure 7B was created by obtaining the moving average of the growth rate in regards to population doubling. Moving averages of three previous data were obtained to smooth out the irregularities seen in this small data set, and to better discern an overall trend.

The initial growth rates kinetics (r of equation 1) showed values of 0.1533/day, 0.1498/day, and 0.1214/day, for hyperpolarized, control, and depolarized cells, respectively. From the growth rate and the values population doubling, it was clear that the change in membrane polarization altered growth kinetics.

Initially, the hyperpolarized cells in pinacidil medium showed a growth rate higher than that of both control and depolarized cells. However, the growth rate of hyperpolarized cells quickly diminished and dramatically lost its ability to proliferate after ~60 days in culture.

Meanwhile, the depolarized cells in high potassium exhibited an overall decline of growth relative to the control cells. Though the depolarized cells grew for a longer period of time, the cumulative average rate of growth was lower than that of control cell lines. Though this cannot be clearly interpreted in figures 3 and 4A, a moving average analysis showed that the moving average growth rate of depolarized cells were lower than that of control cell lines, as seen in figure 4B.

4.4 BrdU Incorporation and Staining Analysis

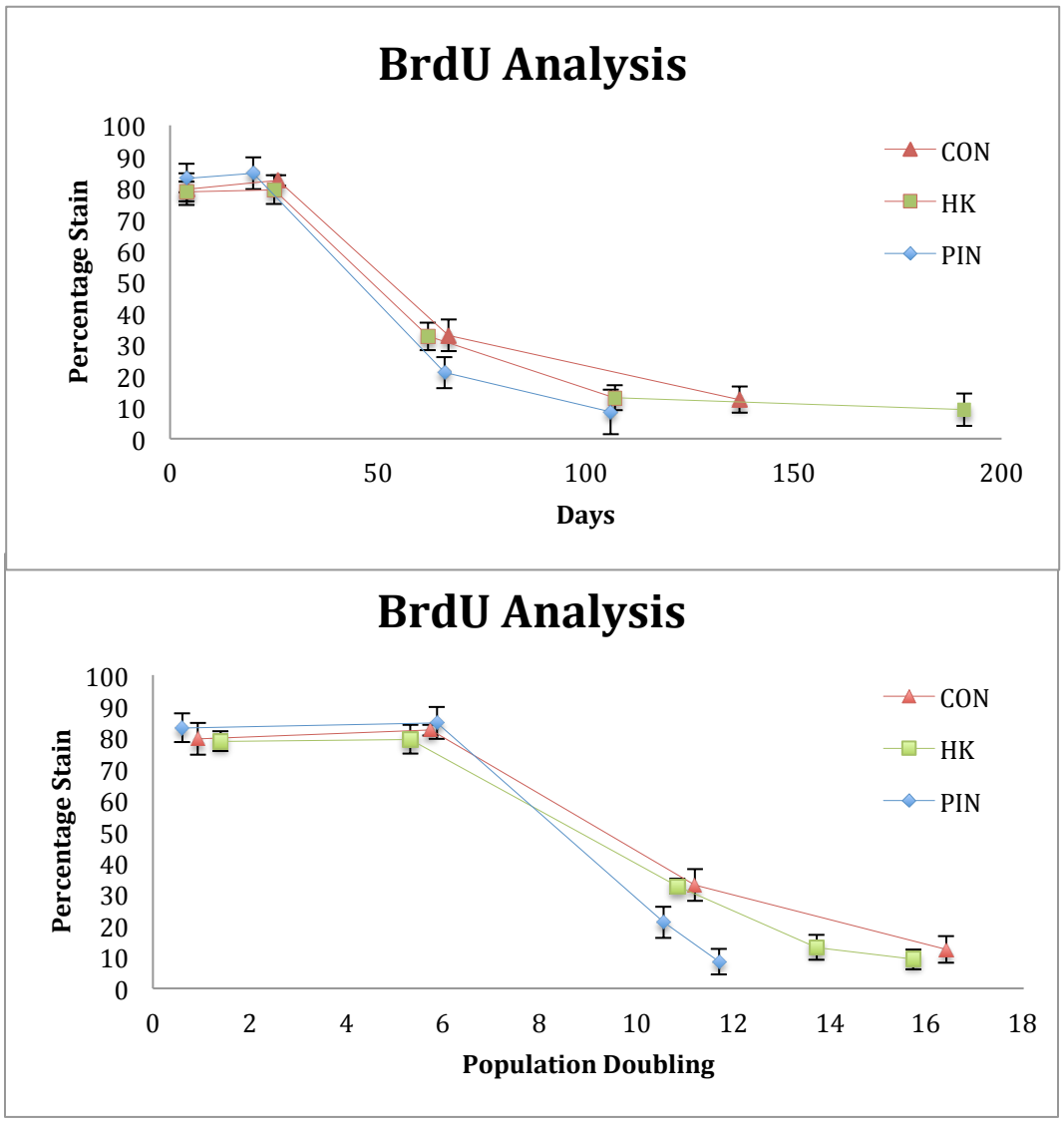

Figure 8 (top) 9 (bottom): *The BrdU incorporation of control (CON), depolarized (HK), and hyperpolarized (PIN) conditions measured against days and population doubling to estimate dividing subpopulations in culture.*

The BrdU incorporation was consistent with the growth rate data, and showed the initial increase in cell division, then the gradual decrease of growth with both time and population doublings. The results of the BrdU

staining in addition to the growth rate data showed how changes in membrane potential affects cell proliferation.

Like the measured growth rates, the maximum growth rate was seen around the fifth passage and the 5-6 PD range for all culture conditions. The BrdU analysis also showed the sharp decrease in staining, and therefore the decrease proliferative potential of hyperpolarized culture past the 5th passage.

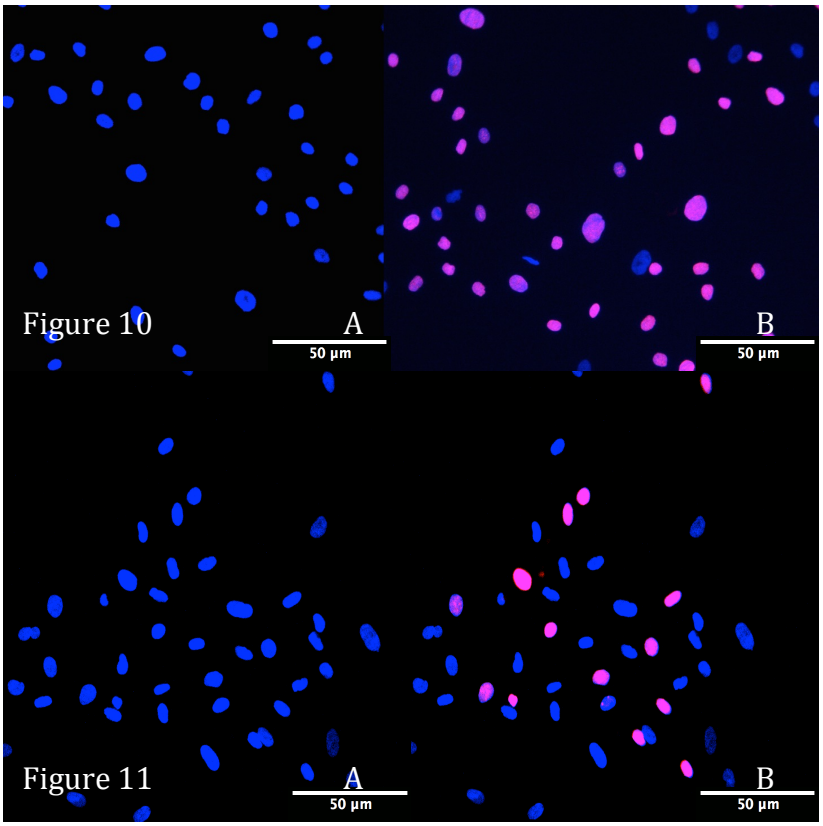

Figure 10/11: *The images above show an example of the BrdU staining conducted in passage 1 (top) and passage 15 (bottom). The left image of figure 10 and 11 were DAPI staining of DNA to show cell numbers, and the right images were stacked images showing degrees of BrdU incorporation.*

4.5 Beta-Galactosidase Senescence Assay

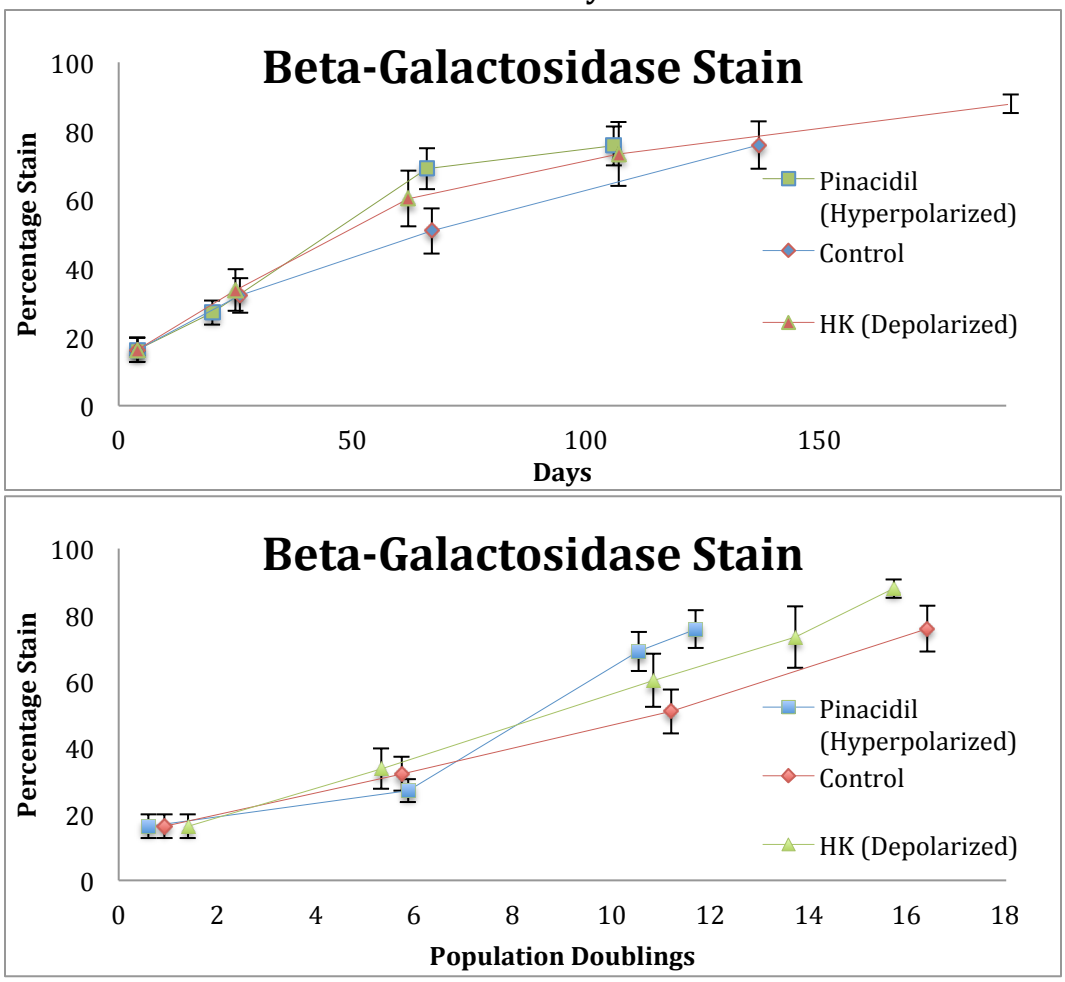

Figure 12 (top) / 13 (bottom): *The images above show the analysis of the incidences of Beta-galactosidase staining through different time points and population doubling.*

As discussed previously, the Beta-galactosidase stain was an assay well correlated to the expression of senescent characteristics. The amount of staining through the different passages was a useful indicator of senescence, and a way to observe how changes in membrane polarization have an effect on the expression of senescence.

Compared to that of the control cell lines, the amount of beta-gal staining was greater in the hyperpolarized and depolarized cell lines. In addition to the incidences of staining, further observations of the images show that the cells grown in membrane modulating media have darker and greater cell area of staining. The results of the beta-gal stain suggested that change in membrane polarization leads to an accelerated onset of senescence. It was hypothesized that the long-term disruption of membrane potential appears to pose a stress on the cells, thereby increasing the percentage of staining in both the depolarized and hyperpolarized culture conditions.

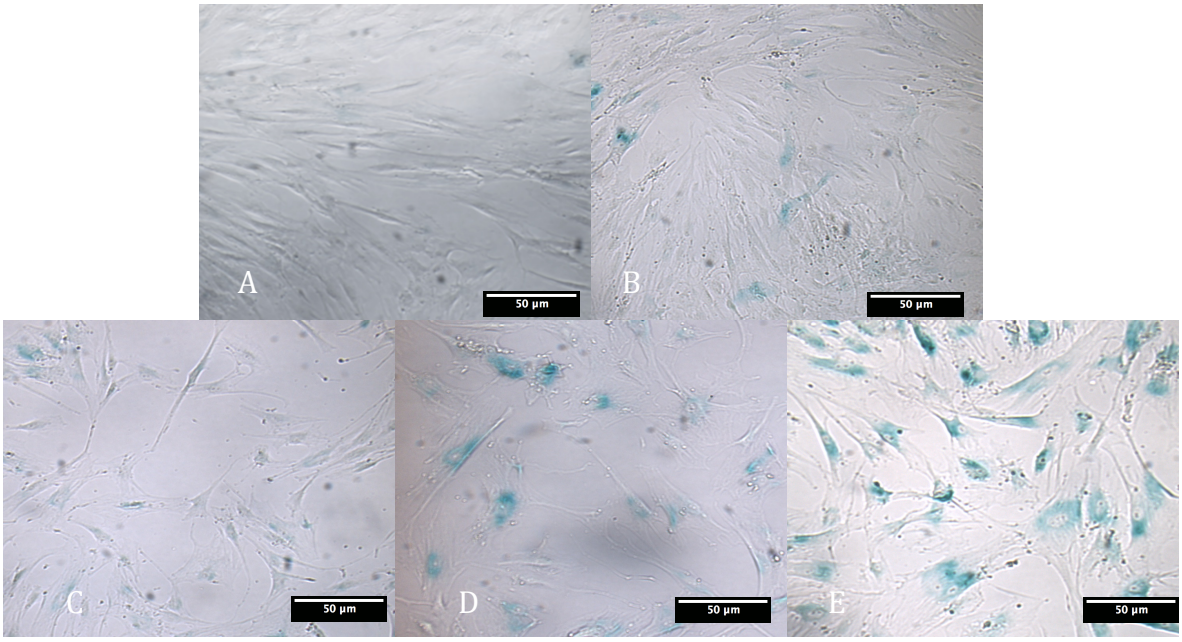

Figure 14-18: *The figures shown above (A-E) are representative images that depict the different degrees of ß-gal staining through different passage numbers. A-E depicts passage numbers 1, 5, 10, 15, and 20, respectively.*

4.6 P53/P21 Analysis

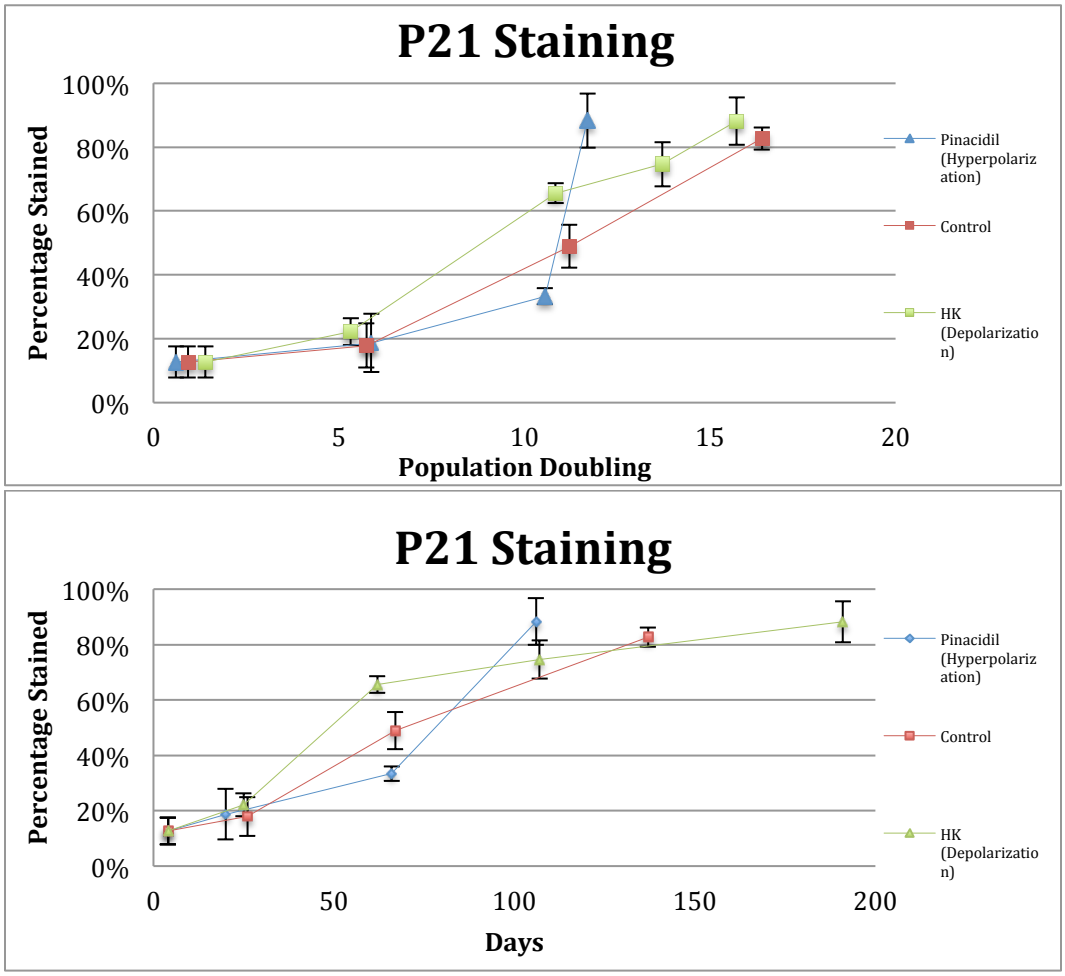

Figure 19/20*: The images above depict the different percentages of P21 (CDKN1A) expression in hyperpolarized, control, and depolarized conditions. As observed in figure 19, the expression of p21 in depolarized MSCs was greater than that of control. The hyperpolarized MSCs showed diminished expression of p21 until around the 11th PD, when it reached replicative senescence.*

The expression of tumor suppressor protein p53 was not observed via immunohistochemistry (IHC) in the cells and passages tested. Two different

sources of p53 antibodies were used, but failed to show expression in the image analysis of IHC procedures. As explained previously, the tumor suppressor protein p53 has high molecular instability due to rapid protease degradation by E3 ubiquitin-protein ligases such as MDM2, MDM4, TOPROS, COP1, and ARF-BP1 (Toledo, 2007). These negative regulators of p53 expression may have made it difficult to observe p53 in IHC. However, contrary to the low and undetectable p53, its downstream protein product cyclin-dependent kinase inhibitor 1 (CDKN1A), or p21, was widely expressed in the hMSCs tested.

Since p21 functions in regulating cell cycle progression at the G1 and S phases, as expected, the incidences of p21 staining increased with greater culture length. The results of staining were in agreement with the calculated growth rate kinetics of the different culture conditions (figure 4), in that the cultures with the highest initial growth rate showed the lowest incidences of p21 staining. This was most clearly illustrated around 50 days, when the percentages of p21 staining between different passages were very distinct.

The earlier hyperpolarized pinacidil cultures, when the highest initial growth rate was observed, showed the lowest amount of p21 staining when compared to that of depolarized and control conditions. However, around 80 days when the hyperpolarized culture also started to show slowed growth, a rapid increase in p21 expression was observed. Corresponding to the lack of proliferation in culture, at 106 days, approximately ~90% of hMSCs in pinacidil medium were stained positive for p21.

The depolarization by high potassium led to an increased overall expression of p21, corresponding to its hampered rate of growth in comparison to control conditions. The amount of p21 staining quickly increased at around 50 days, then increased steadily to around ~90% staining by 191 days, when the culture halted growth.

4.7 P16 Staining Analysis

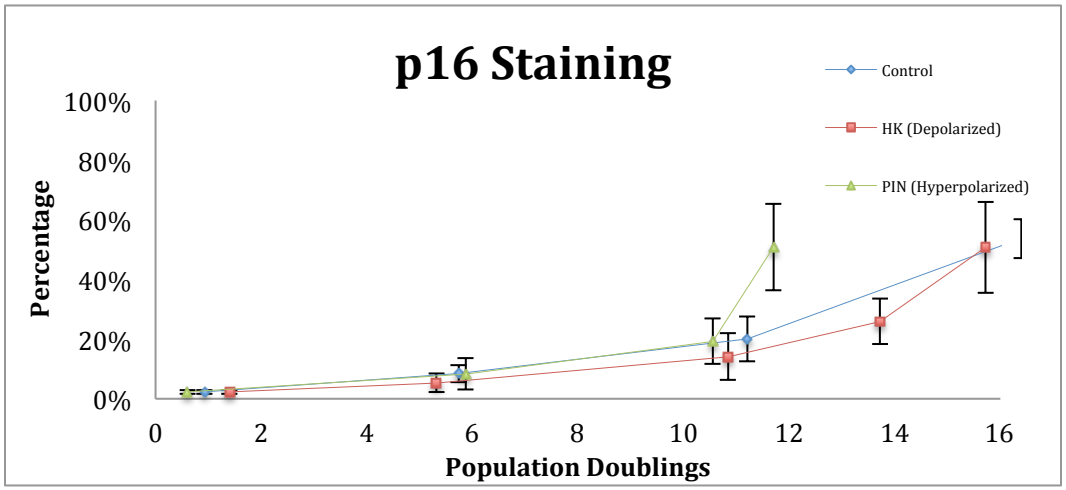

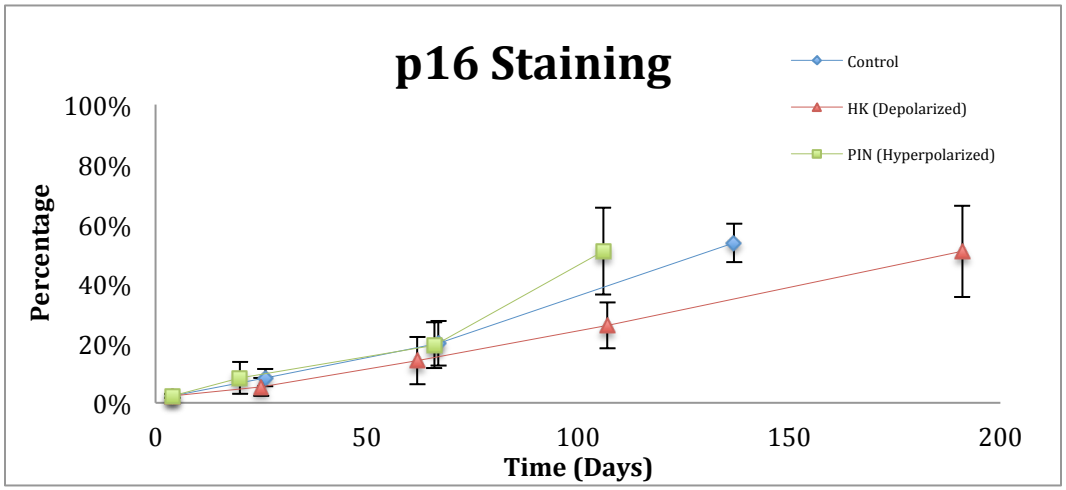

***Figure 21/22**: The images above depict the different percentages of p16 expression through different days and population doublings.*

The p16 staining showed that the percentage of p16 staining increased with population doublings. This was expected as the p16 expression was directly related to the enhancement of cell-cycle suppression elements. Since cell proliferation rates decreased with increase in population, it was natural to see an increase in p16 staining with increasing PD values.

The hyperpolarized pinacidil medium conditions showed a sharp increase in p16 staining between 10.5 and 11.7 PD that corresponded to the rapid cell cycle arrest seen in pinacidil culture. The depolarized and control conditions showed similar formation rates of p16 staining with population doubling, but the depolarized conditions appeared to have lower overall incidences of p16 staining. This could potentially be explained by the affect biophysical control has on the cell cycle transition, specifically the G2/M transition. This was further elaborated upon in section 5.1.1.2 of the discussion.

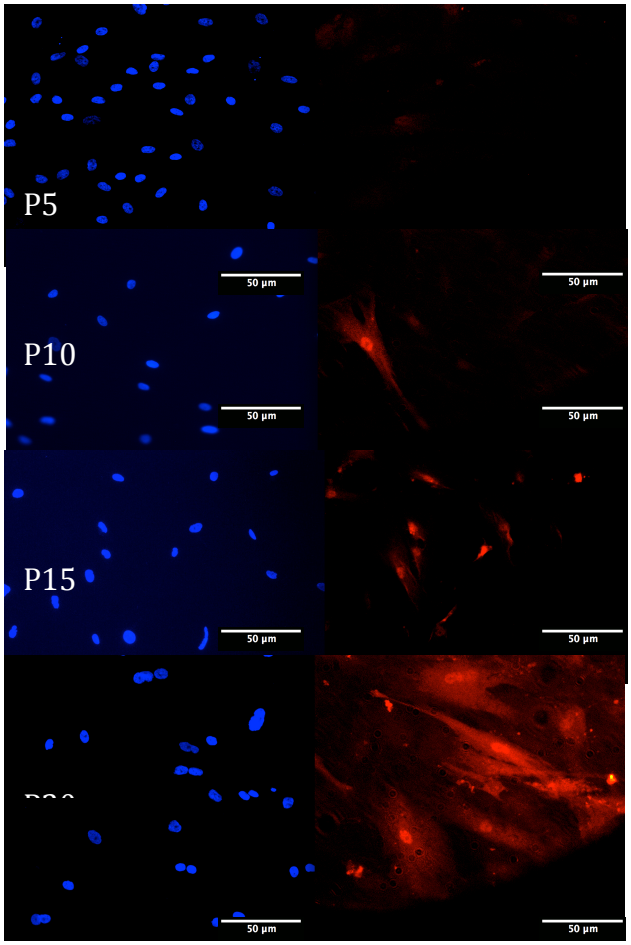

Figure 23-26*: The figures to the left from top to bottom show representative images of the gradual p16 staining in culture in passage 5, 10, 15, and 20.*

4.8 Senescence Associated Heterochromatin Foci (SAHF) Formation

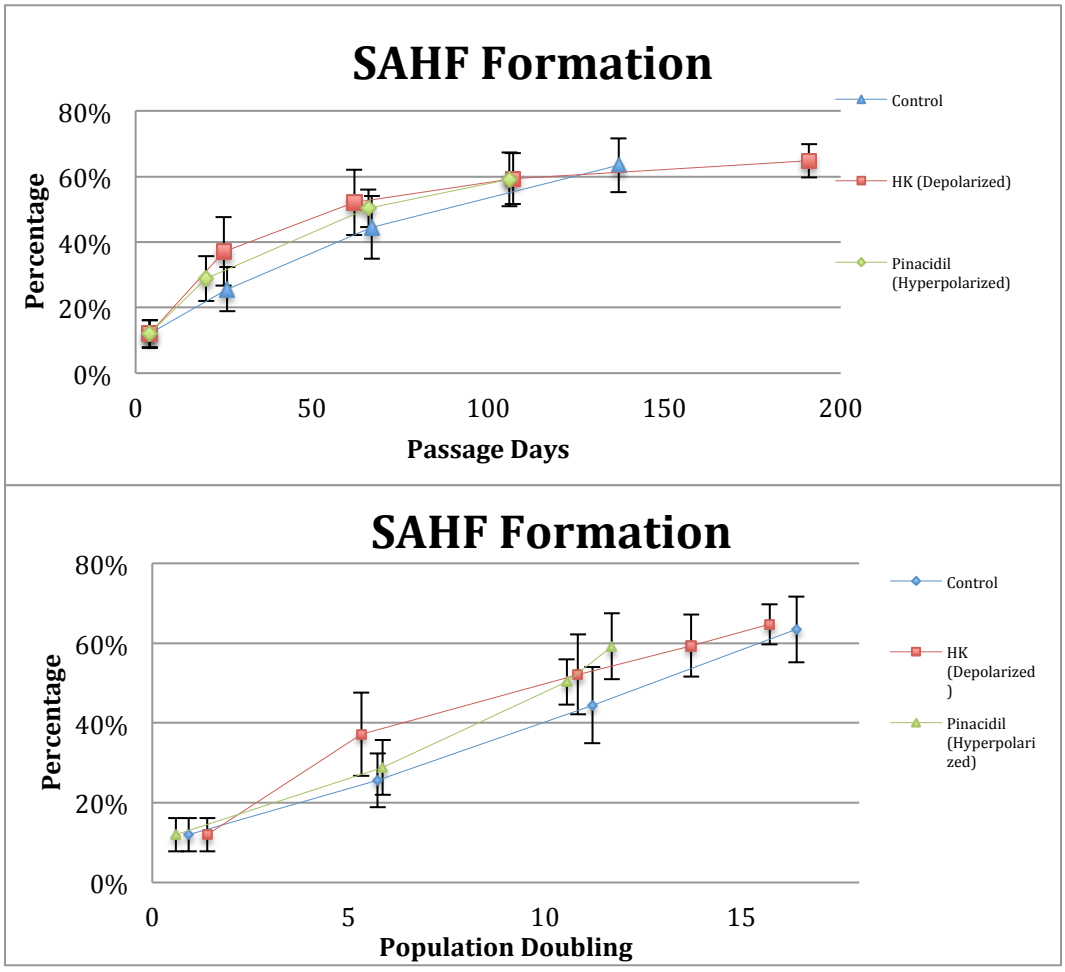

***Figures 27/28**: The above graphs show the different percentages of SAHF formation through different days in culture and population doublings.*

SAHF formation was consistent with the formation of the senescence phenotype. The SAHF formation was higher in the depolarized and hyperpolarized cultures in relation to the control cell line, and reached a maximal formation rates of ~60%. The incidence of SAHF was highest in depolarized cells, suggesting that the depolarization may have a direct consequence in the formation of senescence associate heterochromatin foci. The hyperpolarized condition generally had a higher incidence of

heterochromatin foci formation, but did not exhibit much difference from the control conditions until proliferation arrest, when it exhibited a slight jump in SAHF formation.

Figure 29-32*: The images above show the different amounts of DNA granularity and formation of SAHF through different time points. Images of DAPI stained cells were processed with the gradient magnitude differentials*

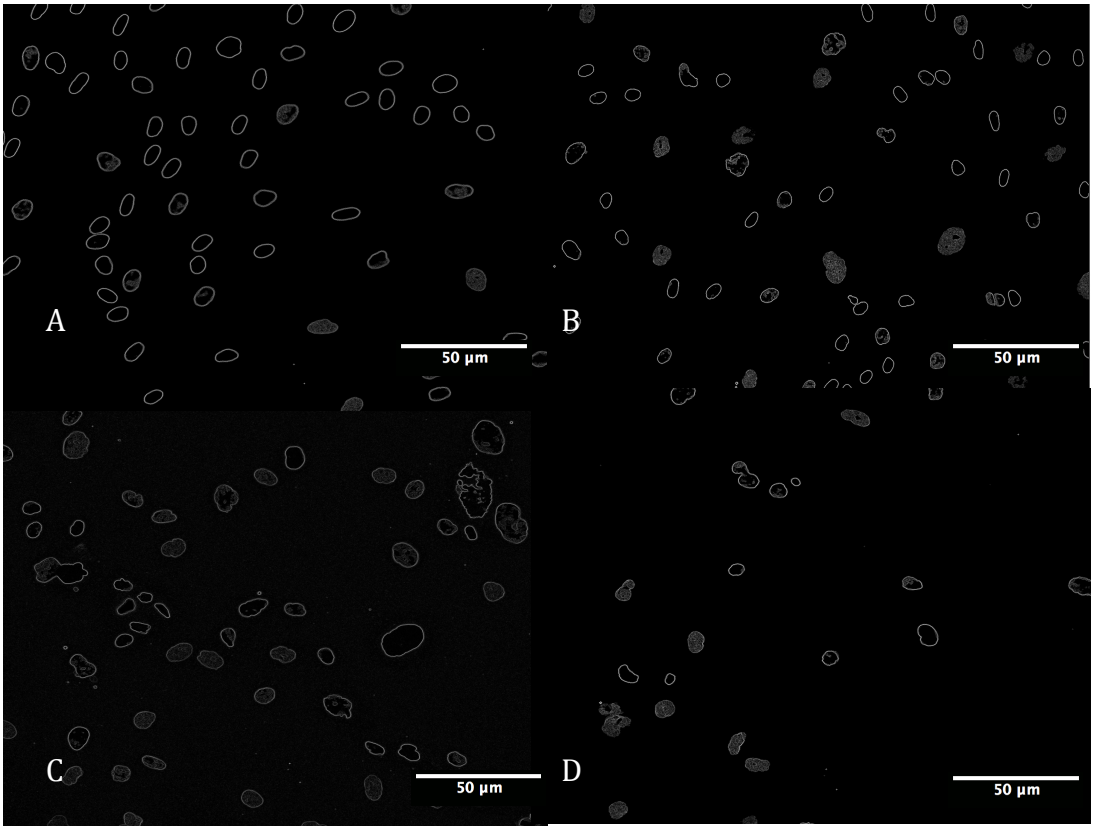

plugin to yield these images. The images A-D show differentials of passages 1, 5, 10 and 15, respectively.

4.9 Relative Telomere Length Analysis (Estimated Telomere Length)

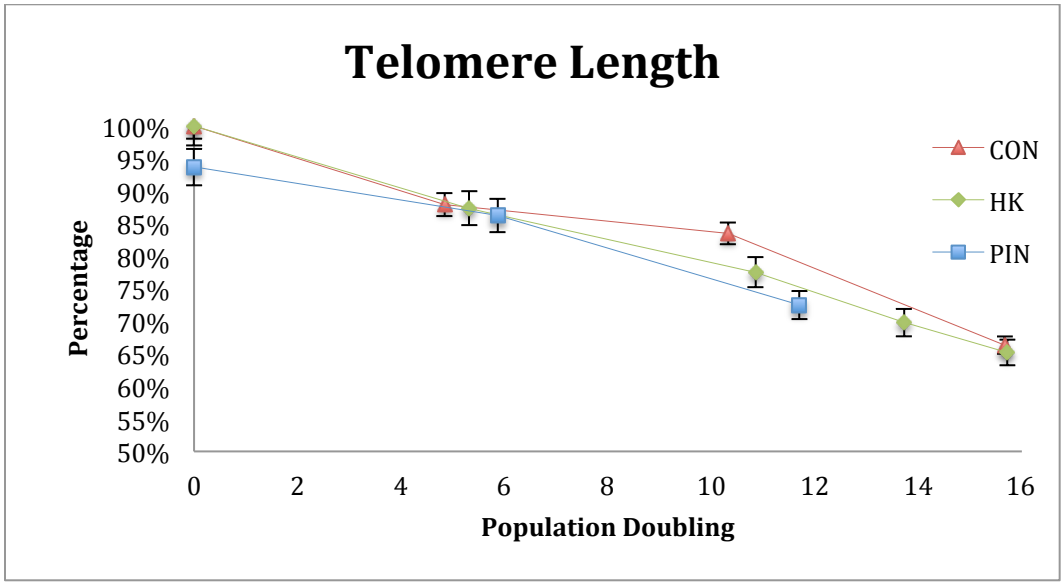

Figure 33: *The graph above shows the change of telomeres through population doublings. The values were obtained by comparing the relative FITC fluorescence intensity of different passages to control cultures.*

The length of telomeres was a rough indicator of how long a cell population divides. In the control and depolarized culture conditions of figure 29, the cells stopped dividing around the same PD and telomere length values. The results of the relative telomere length analysis also showed that depolarization of mesenchymal stem cells did not yield any elongation/preservation of telomere length, and did not preserve a more proliferative state.

The difference in telomere length between the pinacidil conditions and the other culture conditions suggested that the proliferation arrest in the hyperpolarized cells was not the result of just telomere attrition, but other factors. Its premature proliferation arrest may have been result of the stress

the pinacidil medium posed on the cell. The potential reasons behind why/how was further investigated in the discussion.

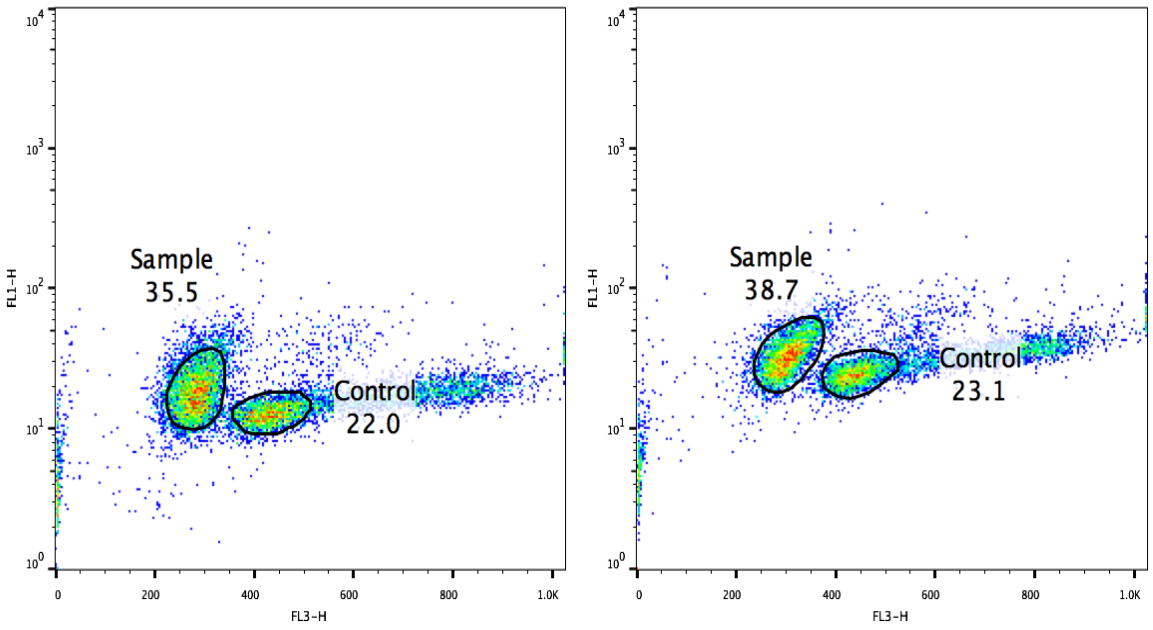

Figure 34/35: *Above are examples of the data analysis and gating processed to acquire relative telomere length values. Figure 30 (left) shows the control conditions without PNA probes, and figure 30 (right) shows the samples with PNA probes. The overall fluorescence intensity as measured in FL1 was clearly higher in that of sample conditions, and this difference was used to measure the relative telomere length values.*

4.10 DiBAC$_4$(3) Staining (Image + Flow Cytometry based)

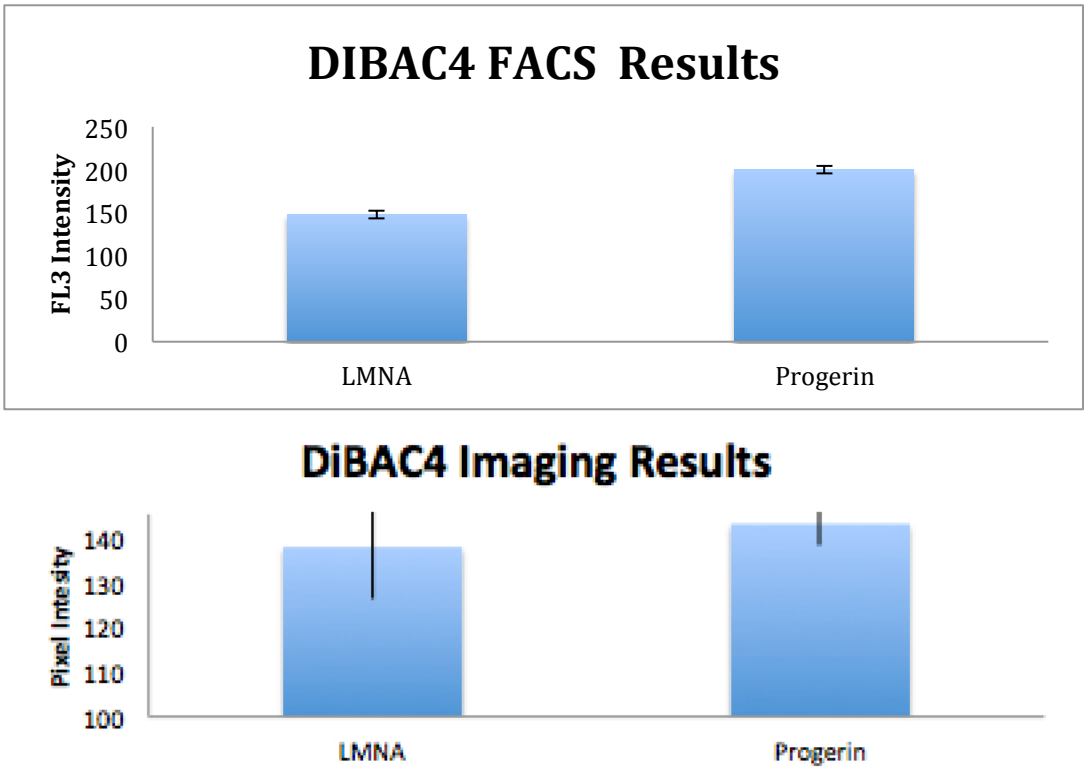

Figure 36/37*: The Images above summarize the results of DiBAC4 image analysis. Figure 32 (above) were results obtained from FACS and figure 33 (below) were results obtained from image analysis.*

Both the image and FACS based analysis showed that a greater amount of DiBAC4 staining was observed in the progerin expressing mesenchymal stem cells. This suggested that the cell membranes of progerin expressing cells were more depolarized than that of the Lamin A expressing control. With the immunofluorescence based imaging, the progerin cells roughly expressed four percent greater DiBAC$_4$ staining than that of the control cells, and in the highthroughput FACS based DIBAC4 staining, we see a 35% increase of fluorescence intensity in progerin cells than the control.

Though specific values of membrane voltage difference could not be obtained from these analyses, the results obtained were important first steps in understanding how Progerin plays an active role in changing membrane potential.

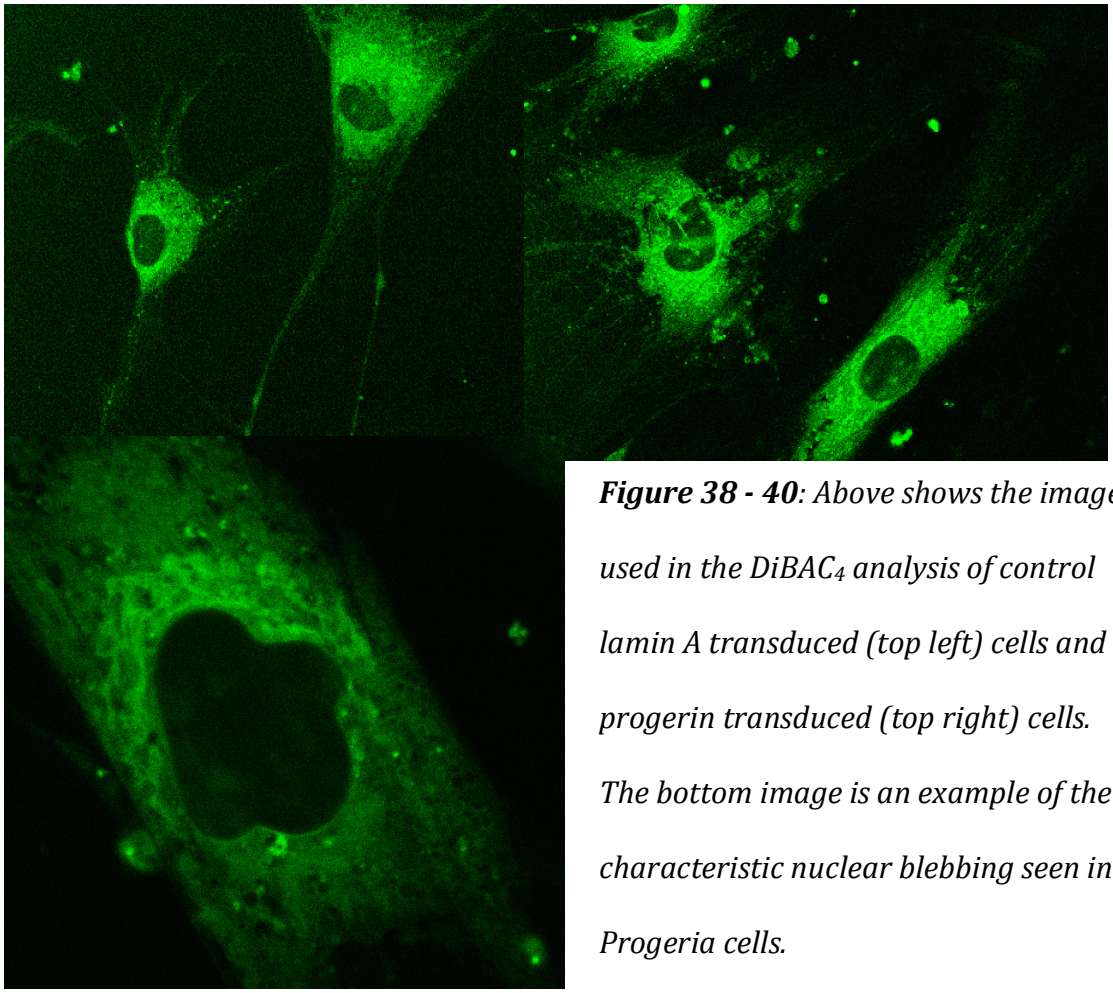

***Figure 38 - 40**: Above shows the images used in the DiBAC$_4$ analysis of control lamin A transduced (top left) cells and progerin transduced (top right) cells. The bottom image is an example of the characteristic nuclear blebbing seen in Progeria cells.*

5.0 Discussion

5.1 Long Term Change in Membrane Potential

From the data collected, it was suggested that the long-term change in membrane potential was not an effective way to foster a more regenerative, proliferative state in mesenchymal stem cells. The long-term culture of hMSCs in membrane potential modulating media appeared to pose a stress on the cell to increase expression of senescence markers. The increase in senescence expression was suggested by the overall increase in beta-galactosidase staining, the increase in SAHF formation, and also the increase in p21 staining in membrane modulating conditions.

Future studies should involve studying how long-term changes in membrane potential affect not just senescence markers, but also other measures of stress. Stress levels could be measured by observing factors such as lipofuscin levels, rate of apoptosis and proteasome activity. In addition, a stress inducing control such as heat shock (32 Celsius incubation) could be compared along side with V_{mem} polarization treatments to see how responses differ.

5.1.1 Cell Cycle Transition and Stress

In the late 60's it was suggested by Clarence D. Cone that the bioelectricity of cells was directly changed through the cell cycle, and that sustained alterations in intracellular ionic concentrations, specifically depolarization, may increase rates of proliferation. There have also been

studies by Chifflet et al. (2003) that showed spontaneous depolarization aided wound healing and growth of epithelial monolayers in culture.

Even with these examples, however, it would be a gross oversimplification to plainly state that depolarization of cells induces cell proliferation. More complicated factors are involved in membrane potential dynamics.

Various studies showed the relationship between the transition of cell cycles and the changing of V_{mem} (Blackiston, 2009). Ion channel dynamics were altered during specific cell cycle transitions, and in the G1/S cycle transition, the V_{mem} was hyperpolarized and in the G2/M cycle transition, the V_{mem} was depolarized. It was possible that the same variation in membrane potential through cell cycles occured with the tested mesenchymal stem cells. This oscillation of voltage membrane potential suggested that temporal variation of membrane modulation could be needed to observe bioelectricity-induced changes in phenotype.

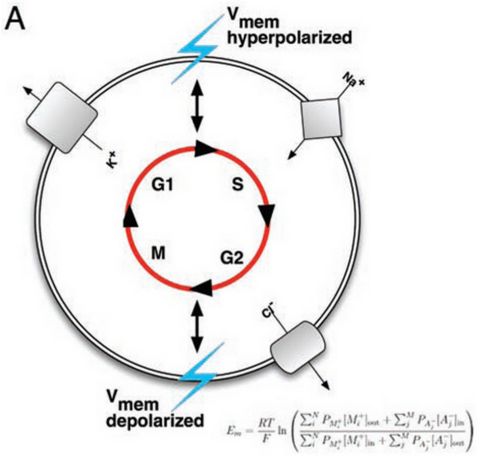

Figure 41*: Figure depicting the difference in membrane polarization through different stages of the cell cycle*

Assigning a single constant value of extracellular ion concentration to induce V_{mem} change may not have been the best method to observe preservation of stem-like characteristics. It was possible that the sustained

long term culture of membrane modulating media may have made cell cycle progression more difficult, thereby leading to the observed altered rates of proliferation and expression of senescence characteristics.

Instead of a single constant value of V_{mem} change, subjecting cells to temporal variations in membrane potential could yield interesting results. For example, culturing cells in depolarizing media for 24 hours, then changing the media with control and/or hyperpolarizing media may yield some interesting results. Work from the Black and Levin labs from Tufts University showed that this strategy was useful for stimulating neonatal cardiomyocyte proliferation in vitro. They observed how depolarization of the resting membrane potential stimulated proliferation of cells (Williams, 2012). Likewise, it is possible that culturing cells in membrane modulating media at the short term could yield interesting results.

5.1.1.1 G1/S Transition

If the same relationship between membrane polarization and cell cycle holds true with hMSCs, it is possible that the depolarization of hMSCs made the progression of G1 to S cell cycle more difficult. In the G1 cycle there is an efflux of K+ ions to make the cell more hyperpolarized and to ready the cells to transition into the S phase. However, due to the extra extracellular K+ ions added, this efflux of K+ ions and membrane hyperpolarization may become more difficult to achieve. This may affect the transition from the G1 to the S phase, in which DNA is replicated. This hypothesis was supported by the results of p21 staining, where we see an increase of staining in

depolarized conditions relative to the other conditions. The p21 protein is a cyclin-dependent kinase inhibitor 1 (CDKN1A) that controls the progression of G1/S cell cycle phases, and a known mediator of cell cycle checkpoint regulation (NCBI, 2014). Therefore, an increase in p21 suggests that the cell cycle transition may have been more controlled/regulated.

Conversely, the hyperpolarization of hMSCs may have made the G1/S transition easier. This is supported by the initial increase in cell growth kinetics observed in pinacidil culture conditions, and also the lowered rates of p21 staining relative to both the control and depolarized conditions.

5.1.1.2 G2/M Transition

Since we see a depolarization of the V_{mem} in G2/M transition in contrast to the G1/S transition, opposing results from the G1/S may be expected in the G2/M transition. The depolarization of cells could allow quicker G2/M transition, while hyperpolarization may result in delayed G2/M phase transition. However, since the G2/M gap acts as a DNA damage checkpoint and ensures that the cells are ‘‘ready’’ to divide and transition to mitosis, an accelerated G2/M transition may be hazardous to the cells, especially at advanced time points. This hypothesis was supported by the calculated cell growth kinetics, and the results of p16 staining.

The hyperpolarized hMSCs experienced an initial upstroke of cell growth rate, possibly due to the truncated time needed in G2/M transition. However, after a certain time, due to the inadequate regulation and inadequate enforcement of the DNA damage checkpoint, we see a sudden cell

cycle arrest at~100 days. The more rapid cell cycle transitions may have led to the cells accumulating greater amounts of genomic damage per population doubling and/or inadequate accumulation of proteins required for G2 and M cell cycles, consequently leading to an abrupt proliferation arrest at G2. This is corroborated by the hyperpolarized cells' increased expression of p16, which induces a more rapid form of senescence through the retinoblastoma pathway than the p53/p21 based responses (Gray-Schopfer, 2006). In addition, the p16-retinoblastoma is known to down regulate a number of genes that encode for proteins that are required in the G2 and M cell cycles (Terada, 2001).

5.2 Preservation of Regeneration

Another interpretation of the slow growth rate induced by depolarization could be that it is a way to slow the onset of senescence by limiting growth. Stem cell overproliferation may lead to exhaustion of the stem cell pool, resulting in fewer stem cells available for healing/regeneration. The slowed growth rate via depolarization could potentially be a way to preserve cells so that they grow for a longer time, but without exhaustion of the dividing stem cell population. Due to the lowered growth rate, the point of cellular senescence maybe delayed, thereby elongating lifespan.

5.3 Future Directions and Matters of Interest – Senescence

5.3.1 Temporal Variation in Membrane Voltage Modulation

Since it was observed here that long-term change in membrane potential does not diminish the characteristics of senescence, the next steps should involve temporal variations in membrane voltage modulation. To better understand the effect of depolarization on human mesenchymal stem cells, it may be better to induce more acute treatments of depolarization. A short-term culture of membrane modulating medium may be a better way to elucidate how alteration of voltage membrane potential may affect senescence.

5.3.2 Observation of Stemness

An important next step for this study would be to investigate the effect of membrane potential modulation on stemness, the differentiation capacity of the cells.

To study the stemness, hMSCs should be grown to different passages in control media, and then treated with temporal variations (e.g. 3 hours, 12 hours, 24 hours) of membrane potential modulating agents. Following the treatments of membrane potential modulation, the cells will then be differentiated to osteogenic and adipogenic cells to observe the expression of the respective differentiation characteristics.

Studies by Breudigam et al. (2010) suggested that older stem cells have lesser capacity to differentiate into bone cells, and would be more inclined to differentiate to fat. Therefore, if the short-term culture of hMSCs

is successful in inducing characteristics of a more pre-proliferative state, it is hypothesized that the depolarized conditions would allow for greater differentiation of mesenchymal stem cells into bone.

5.3.3 G2/M Transition Marker

In addition, a marker for G2/M transition such as a phosphorylated-histone H3 could be a good way to investigate the hypothesis of how depolarization hastens G2/M transition and how hyperpolarization slows it (Zeitlin, 2001). If the hypothesis is correct, depolarization should show decreased and hyperpolarization should show an increased expression of phosphor-histone H3.

5.4 Biophysical Characteristics and Progeria

An increase in fluorescence intensity was seen in the hMSCs transduced with the progerin gene versus the hMSCs with transduced lamin-A genes. This suggested that an active change in membrane potential could be occurring with the expression of progerin. The higher fluorescence intensity pointed to the possibility that progerin expressing hMSCs had more depolarized resting membrane potential.

This was contrary to what was expected in these tests. It was hypothesized that due to its characteristics of accelerated aging, Progerin expressing cells may show more hyperpolarization compared to control cells. To verify the results of these tests for the future, this study will require longer observational time---points for cell growth comparing progerin+/--- cells and also direct observations of this change to membrane potential.

It was also possible that the difference in fluorescence may have been the result of poor cell health and sensitivity to the toxic $DiBAC_4(3)$ dye, and not strictly the membrane voltage depolarization. Since progerin expression leads to the instability of the nucleus and is characterized by greater rates of apoptosis and dynsfunction (Pollex, 2004), it was possible that the progerin expressing cells had greater sensitivity towards the $DiBAC_4(3)$ dye. In the $DiBAC_4(3)$ image analysis, it was observed that greater incidences of partial cell detachment occurred during $DiBAC_4(3)$ treatment. These points of detachment, as observed in figure 42/43, created bright speckles of staining that may have increased the average pixel intensity results.

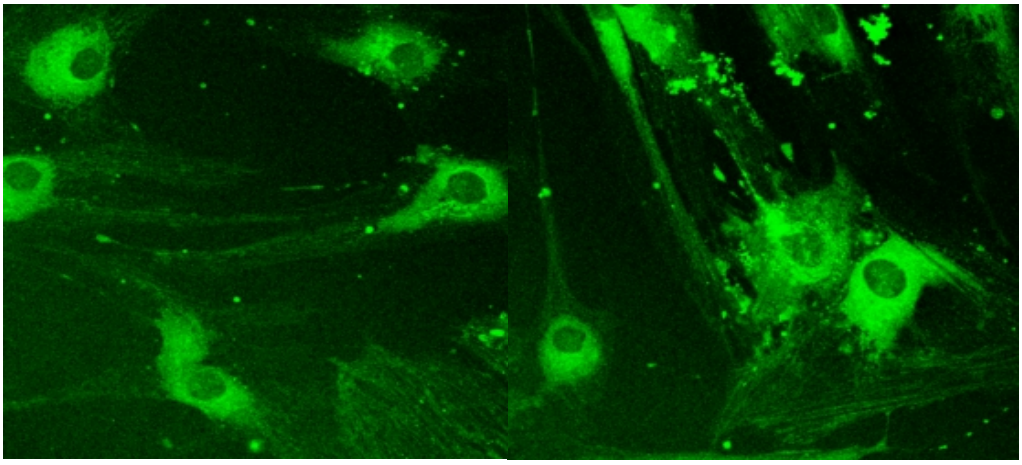

Figure 42 – 43*: Figure 42 (left) shows the $DiBAC_4(3)$ image analysis of the transduced Lamin A control cells, and figure 43 (right) shows progerin gene transduced cells. The greater incidences of speckling may have played a role in showing higher intracellular concentrations of $DiBAC_4(3)$.*

5.5 Limitations/Difficulty with Progeria cells

Due to its nuclear fragility, progerin positive cells have increased apoptotic cell death and reduced stem cell growth (Halaschek-Wiener, 2007). The apoptotic death and low growth rate of the Progerin-expressing mesenchymal stem cell line made it impractical to replicate the same type of long-term depolarization/hyperpolarization senescence studies the Progeria project. Other alternative cell source options such as progerin-expressing fibroblasts were tested and found to grow more quickly, but correspondingly lacked the characteristic progerin expression. Important hallmarks of Progeria such as nuclear blebbing were absent in the fibroblasts. Therefore, smaller scale studies of biophysical characteristics through $DiBAC_4(3)$ staining were pursued.

5.6 Future Directions – Progeria Project

Though HGPS cells naturally lack the capacity to proliferate widely, recent work with human induced pluripotent stem cell (iPSC) technology showed greater promise of replicating the disease in vitro. The iPSCs prior to differentiation lack the characteristics of regular Progeria cells, which allows the higher proliferation and collection of cells (Miller, 2013). This provides a platform and greater flexibility for in vitro testing of Progeria cells. Future studies with Progeria should involve the effect modulation of biophysical signaling affects the expression of Progeria characteristics during/after differentiation into osteogenic and adipogenic cell lines.

Future studies with Progeria should involve the effect modulation of biophysical signaling affects the expression of Progeria characteristics during/after differentiation into osteogenic and adipogenic cell lines.

6.0 Conclusions

From the data collected, it was concluded that long term changes in membrane potential does not recapitulate a cell's pre-senescent state or diminish expression of senescence characteristics. It was hypothesized that the sustained culture of the cells in a single constant value of V_{mem} may have made cell cycle progression more difficult, thereby leading to the altered rates of proliferation and changes in the expression of senescence characteristics.

Further studies should involve temporal variations in membrane potential to observe how the variation in V_{mem} alters the expression of senescence, and perhaps recapitulate a cell's more pre-senescent state.

In addition, the results of the $DiBAC_4(3)$ staining of Progeria cells were promising. The dramatic change in depolarization seen in the FACS based DiBAC4 staining suggested that a direct change in voltage membrane occurs with progerin expression. This may suggest that short-term changes in membrane potential may be directed to modulate disease progression kinetics.

References

Adams, P. D. (2007). Remodeling of chromatin structure in senescent cells and its potential impact on tumor suppression and aging. *Gene*.

Adams, P. D. (2009). Healing and hurting: molecular mechanisms, functions, and pathologies of cellular senescence. *Molecular cell*.

Bartkova, J., Rezaei, N., Liontos, M., Karakaidos, P., Kletsas, D., Issaeva, N., et al. (2006). Oncogene---induced senescence is part of the tumorigenesis barrier imposed by DNA damage checkpoints. *Nature*, *444*(7119), 633–637. doi:10.1038/nature05268

Beane, W. S., Morokuma, J., Adams, D. S., & Levin, M. (2011). A Chemical Genetics Approach Reveals H,K---ATPase---Mediated Membrane Voltage Is Required for Planarian Head Regeneration. *Chemistry & Biology*, *18*(1), 77–89. doi:10.1016/j.chembiol.2010.11.012

Brady, C. A., Jiang, D., Mello, S. S., Johnson, T. M., & Jarvis, L. A. (2011). Distinct p53 transcriptional programs dictate acute DNA---damage responses and tumor suppression. *Cell*.

Burtner, C. R., & Kennedy, B. K. (2010b). Progeria syndromes and ageing: what is the connection?, 1–12. doi:10.1038/nrm2944

Campisi, J. (2001). Cellular senescence as a tumor---suppressor mechanism. *Trends in cell biology*.

Campisi, J. (2005). Senescent Cells, Tumor Suppression, and Organismal Aging: Good Citizens, Bad Neighbors. *Cell*, *120*(4), 513–522. doi:10.1016/j.cell.2005.02.003

Campisi, J., & di Fagagna, F. A. (2007). Cellular senescence: when bad things happen to good cells. *Nature reviews Molecular cell biology*.

Celli, G. B., & de Lange, T. (2005). DNA processing is not required for ATM---mediated telomere damage response after TRF2 deletion. *Nature Cell Biology*, *7*(7), 712–718. doi:10.1038/ncb1275

Cha, B.---H., Lee, J.---S., Kim, S. W., Cha, H.---J., & Lee, S.---H. (2013). The modulation of the oxidative stress response in chondrocytes by Wip1 and its effect on senescence and dedifferentiation during in vitro expansion. *Biomaterials*, *34*(9), 2380–2388. doi:10.1016/j.biomaterials.2012.12.009

Chang, S.---W., Chang, G.---J., & Su, M.---J. (2006). Change of Potassium Current Density in Rabbit Corneal Epithelial Cells During Maturation and Cellular Senescence. *Journal of the Formosan Medical Association*, *105*(1), 7–16. doi:10.1016/S0929---6646(09)60103---0

Chen, Q. (2001). Uncoupling the Senescent Phenotype from Telomere Shortening in Hydrogen Peroxide---Treated Fibroblasts. *Experimental Cell Research*, *265*(2), 294–303. doi:10.1006/excr.2001.5182

Cheng, N., Van Hoof Harry, Bocky, E., & De Loecker, W. (2004). Effects of Electric Currents on ATP Generation, Prothein Synthesis, and Membrane Transport in Rat Skin, 1–8.

Chifflet, S., & Hernández, J. A. (2005). A possible role for membrane depolarization in epithelial wound healing. *American Journal of …*.

Chifflet, S., Hernández, J. A., Grasso, S., & Cirillo, A. (2003). Nonspecific depolarization of the plasma membrane potential induces cytoskeletal modifications of bovine corneal endothelial cells in culture. *Experimental Cell Research*.

Cone, C. D., Jr. (1970). Variation of the transmembrane potential level as a basic mechanism of mitosis control. *Oncology*.

d'Adda di Fagagna, F. (2008). Living on a break: cellular senescence as a DNA---damage response. *Nature Reviews Cancer*, *8*(7), 512–522. doi:10.1038/nrc2440

Denchi, E. L., & de Lange, T. (2007). Protection of telomeres through independent control of ATM and ATR by TRF2 and POT1. *Nature*, *448*(7157), 1068–1071. doi:10.1038/nature06065

Downey, M., & Durocher, D. (2006). gammaH2AX as a checkpoint maintenance signal. *CELL CYCLE---LANDES …*.

Estrada, J. C., Torres, Y., a, A. B. I., Dopazo, A., Roche, E., Carrera---Quintanar, L., et al. (2013). Human mesenchymal stem cell---replicative senescence and oxidative stress are closely linked to aneuploidy, *4*(6), e691–13. doi:10.1038/cddis.2013.211

Galluzzi, L., Vitale, I., Kepp, O., & Kroemer, G. (2013). *Cell Senescence*. Humana Press.

Gan, W., Ben Nie, Shi, F., Xu, X.---M., Qian, J.---C., Takagi, Y., et al. (2012). Age---dependent increases in the oxidative damage of DNA, RNA, and their metabolites in normal and senescence---accelerated mice analyzed by LC–

MS/MS: Urinary 8---oxoguanosine as a novel biomarker of aging. *Free Radical Biology and Medicine*, *52*(9), 1700–1707. doi:10.1016/j.freeradbiomed.2012.02.016

Gray---Schopfer, V. C., Cheong, S. C., Chong, H., Chow, J., Moss, T., Abdel---Malek, Z. A., et al. (2006). Cellular senescence in naevi and immortalisation in melanoma: a role for p16? *British Journal of Cancer*, *95*(4), 496–505. doi:10.1038/sj.bjc.6603283

HAYFLICK, L., JACOBS, P., & PERKINS, F. (1964). A Procedure for the Standardization of Tissue Culture Media. *Nature*, *204*(4954), 146–147. doi:10.1038/204146a0

Hennekam, R. C. M. (2006). Hutchinson–Gilford progeria syndrome: Review of the phenotype. *American Journal of Medical Genetics Part A*, *140A*(23), 2603–2624. doi:10.1002/ajmg.a.31346

Huang, Y., Zhang, H., Yang, S., Qiao, H., Zhou, W., & Zhang, Y. (2012). Liuwei Dihuang decoction facilitates the induction of long---term potentiation (LTP) in senescence accelerated mouse/prone 8 (SAMP8) hippocampal slices by inhibiting voltage---dependent calcium channels (VDCCs) and promoting N---methyl---d---aspartate receptor (NMDA) receptors. *Journal of Ethnopharmacology*, *140*(2), 384–390. doi:10.1016/j.jep.2012.01.030

Jin, M., Inoue, S., Umemura, T., Moriya, J., & Arakawa, M. (2001). Cyclin D1, p16 and retinoblastoma gene product expression as a predictor for prognosis in non---small cell lung cancer at stages I and II. *Lung Cancer*.

Joaquin, A., & Fernandez---Capetillo, O. (2012). Signalling DNA Damage. InTech. doi:10.5772/50863

Kim, M. J., Kim, C. W., Choi, Y. S., Kim, M. H., & Park, C. J. (2012). … ---related alterations in mesenchymal stem cells related to shift in differentiation from osteogenic to adipogenic potential: implication to age---associated bone diseases …. *Mechanisms of ageing …*.

Kim, W. Y., & Sharpless, N. E. (2006). The Regulation of INK4/ ARF in Cancer and Aging. *Cell*.

Kosar, M., Bartkova, J., Hubackova, S., & Hodny, Z. (2011). Senescence---associated heterochromatin foci are dispensable for cellular senescence, occur in a cell type---and insult---dependent manner and follow expression …. *Cell*.

Kuilman, T., Michaloglou, C., Mooi, W. J., & Peeper, D. S. (2010). The essence of senescence. *Genes & Development*, *24*(22), 2463–2479.

doi:10.1101/gad.1971610

Kurz, D. J., Decary, S., & Hong, Y. (2000). Senescence---associated (beta)---galactosidase reflects an increase in lysosomal mass during replicative ageing of human endothelial cells. *Journal of Cell …*.

Larsson, L.---G. (2011a). Oncogene--- and tumor suppressor gene---mediated suppression of cellular senescence. *Seminars in Cancer Biology*, *21*(6), 367–376. doi:10.1016/j.semcancer.2011.10.005

Larsson, L.---G. (2011b). Cellular senescenceâ€"A barrier against tumor development? *Seminars in Cancer Biology*, *21*(6), 347–348. doi:10.1016/j.semcancer.2011.11.001

Lawless, C., Wang, C., Jurk, D., Merz, A., Zglinicki, von, T., & Passos, J. F. (2010). Quantitative assessment of markers for cell senescence. *EXG*, *45*(10), 772–778. doi:10.1016/j.exger.2010.01.018

Lee, B. Y., Han, J. A., Im, J. S., Morrone, A., & Johung, K. (2006). Senescence---associated β---galactosidase is lysosomal β---galactosidase. *Aging Cell*.

Levin, M. (2012). Morphogenetic fields in embryogenesis, regeneration, and cancer: Non---local control of complex patterning. *BioSystems*, *109*(3), 243–261. doi:10.1016/j.biosystems.2012.04.005

Levin, M., & Stevenson, C. G. (2012). Regulation of cell behavior and tissue patterning by bioelectrical signals: challenges and opportunities for biomedical engineering. *… review of biomedical engineering*.

Liu, G.---H., Barkho, B. Z., Ruiz, S., Diep, D., Qu, J., Yang, S.---L., et al. (2011). Recapitulation of premature ageing with iPSCs from Hutchinson---Gilford progeria syndrome. *Nature*, *472*(7342), 221–225.

López---Otín, C., Blasco, M. A., Partridge, L., Serrano, M., & Kroemer, G. (2013). The Hallmarks of Aging. *Cell*, *153*(6), 1194–1217. doi:10.1016/j.cell.2013.05.039

Miller, J. D., Ganat, Y. M., Kishinevsky, S., Bowman, R. L., Liu, B., Tu, E. Y., et al. (2013). Human iPSC---Based Modeling of Late---Onset Disease via Progerin---Induced Aging. *Stem Cell*, *13*(6), 691–705. doi:10.1016/j.stem.2013.11.006

Narita, M., Nuñez, S., Heard, E., Narita, M., & Lin, A. W. (2003). Rb---mediated heterochromatin formation and silencing of E2F target genes during cellular senescence. *Cell*.

Prokocimer, M., Barkan, R., & Gruenbaum, Y. (2013b). Hutchinson---Gilford progeria syndrome through the lens of transcription. *Aging Cell*, *12*(4), 533–543. doi:10.1111/acel.12070

Ramirez, R. D., Morales, C. P., & Herbert, B. S. (2001). Putative telomere---independent mechanisms of replicative aging reflect inadequate growth conditions. *Genes & …*.

Robbins, E., Levine, E. M., & Eagle, H. (1970). Morphologic changes accompanying senescence of cultured human diploid cells. *The Journal of experimental …*.

Rufini, A., Tucci, P., Celardo, I., & Melino, G. (2013). Senescence and aging: the critical roles of p53, *32*(43), 5129–5143. doi:10.1038/onc.2012.640

Sundelacruz, S., & Kaplan, D. L. (2009). Stem cell--- and scaffold---based tissue engineering approaches to osteochondral regenerative medicine. *Seminars in Cell & Developmental Biology*, *20*(6), 646–655. doi:10.1016/j.semcdb.2009.03.017

Toledo, F., & Wahl, G. M. (2007). MDM2 and MDM4: p53 regulators as targets in anticancer therapy. *The international journal of biochemistry & cell biology*, *39*(7), 1476–1482.

Tollefsbol, T. O. (2007). *Biological Aging*. Springer Science & Business Media.

Urquidi, V., Tarin, D., & Goodison, S. (2000). Role of telomerase in cell senescence and oncogenesis. *Annual review of medicine*.

Vijg, J. (2009). SNP'ing for longevity. *Aging*.

Wagner, W. (2010). Senescence is heterogeneous in mesenchymal stromal cells – kaleidoscopes for cellular aging. *Cell Cycle*, *9*(15), 2923–2924. doi:10.4161/cc.9.15.12741

Wang, J. (2014). SIRT1 ameliorates age---related senescence of mesenchymal stem cells via modulating telomere shelterin, 1–12. doi:10.3389/fnagi.2014.00103/abstract

Worman, H. J., & Courvalin, J. C. (2004). How do mutations in lamins A and C cause disease? *Journal of Clinical Investigation*.

Yang, Q., Zheng, Y. L., & Harris, C. C. (2005). POT1 and TRF2 Cooperate To Maintain Telomeric Integrity. *Molecular and Cellular Biology*, *25*(3), 1070–1080. doi:10.1128/MCB.25.3.1070---1080.2005

Zhang, J., Lian, Q., Zhu, G., Zhou, F., Sui, L., & Tan, C. (2011). A human iPSC model of Hutchinson Gilford Progeria reveals vascular smooth muscle and mesenchymal stem cell defects. *Cell stem cell*.